Chroman-4-one- and Chromone-Based Sirtuin 2 Inhibitors with Antiproliferative Properties in Cancer Cells

Seifert, Tina

American Chemical Society
2014-12-11

Seifert, T, Malo, M, Kokkola, T, Engen, K, Friden-Saxin, M, Wallen, E A A, Lahtela-Kakkonen, M, Jarho, E M & Luthman, K 2014, 'Chroman-4-one- and Chromone-Based Sirtuin 2 Inhibitors with Antiproliferative Properties in Cancer Cells', Journal of Medicinal Chemistry, vol. 57, no. 23, pp. 9870-9888. https://doi.org/10.1021/jm500930h

http://hdl.handle.net/10138/224458
10.1021/jm500930h

other
publishedVersion

Journal of Medicinal Chemistry

Article

pubs.acs.org/jmc

Chroman-4-one- and Chromone-Based Sirtuin 2 Inhibitors with Antiproliferative Properties in Cancer Cells

Tina Seifert,[†] Marcus Malo,[†] Tarja Kokkola,[‡] Karin Engen,[†] Maria Fridén-Saxin,[†] Erik A. A. Wallén,[§] Maija Lahtela-Kakkonen,[‡] Elina M. Jarho,*[,‡] and Kristina Luthman*[,†]

[†]Department of Chemistry and Molecular Biology, Medicinal Chemistry, University of Gothenburg, Kemivagen 10, SE-412 96 Göteborg, Sweden

[‡]School of Pharmacy, University of Eastern Finland, P.O. Box 1627, 70211 Kuopio, Finland

[§]Division of Pharmaceutical Chemistry and Technology, Faculty of Pharmacy, University of Helsinki, FIN-00014 Helsinki, Finland

Supporting Information

ABSTRACT: Sirtuins (SIRTs) catalyze the NAD^+-dependent deacetylation of N^{ε}-acetyl lysines on various protein substrates. SIRTs are interesting drug targets as they are considered to be related to important pathologies such as inflammation and aging-associated diseases. We have previously shown that chroman-4-ones act as potent and selective inhibitors of SIRT2. Herein we report novel chroman-4-one and chromone-based SIRT2 inhibitors containing various heterofunctionalities to improve pharmacokinetic properties. The compounds retained both high SIRT2 selectivity and potent inhibitory activity. Two compounds were tested for their antiproliferative effects in breast cancer (MCF-7) and lung carcinoma (A549) cell lines. Both compounds showed antiproliferative effects correlating with their SIRT2 inhibition potency. They also increased the acetylation level of α-tubulin, indicating that SIRT2 is likely to be the target in cancer cells. A binding mode of the inhibitors that is consistent with the SAR data was proposed based on a homology model of SIRT2.

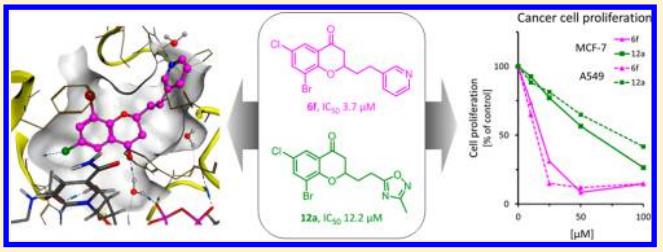

INTRODUCTION

Sirtuins (SIRTs) compose class III of lysine deacetylases (KDACs). There are seven conserved human isoforms (SIRT1−SIRT7) with different subcellular locations.[1] The enzymes catalyze the reversible deacetylation of lysine residues both on histones (H1, H3, H4) and nonhistone proteins, e.g., p53, p65, PGC-1α, PPARγ, FOXO, NFκB, and α-tubulin.[2] The deacetylation reaction requires nicotinamide adenine dinucleotide (NAD^+) as cosubstrate, and results in the formation of the deacetylated protein substrate, *O*-acetyl-ADP-ribose, and nicotinamide, which is the endogenous inhibitor of the sirtuins.[3−5] In addition to the deacetylation, also mono-ADP-ribosyl transferase activity and removal of long-chain fatty acyl groups from lysine residues have been reported for SIRT6.[6−8] Mono-ADP-ribosyl transferase activity is the only effect observed for SIRT4.[9] Recently, Du et al. discovered lysine demalonylation and desuccinylation activities of SIRT5,[10] which later was followed by reports by Zhao and co-workers regarding deglutarylation from lysine residues as a function of SIRT5.[11]

Because of the broad spectrum of substrates, SIRTs have been implicated as regulators in a range of physiological processes, including metabolism, cell survival and apoptosis, gene expression, and DNA repair.[12] Therefore, the enzymes have been proposed to be involved in pathologies such as inflammation and aging-associated diseases, e.g., cancer, diabetes, and neurodegeneration (e.g., Alzheimer's, Huntington's, and Parkinson's disease).[13,14] The potent SIRT1 inhibitor selisistat (**36** (Ex-527), Chart 2) reduces Huntington's disease pathology[15] and has been in phase II clinical studies.[16]

SIRT2, which is the focus of the present study, is predominantly located in the cytoplasm but is enriched in the nucleus during mitosis.[17] Beside the deacetylation of histone H4, the enzyme is also involved in the deacetylation of nonhistone substrates such as α-tubulin, FOXO, p65, p300, and p53.[18] Hence, the enzyme is proposed to be involved in the regulation of the cell cycle.[19]

SIRT2 is highly expressed in the brain,[18] and inhibition appears to be neuroprotective as two SIRT2 selective inhibitors have been shown to counteract progression of Huntington's[20,21] and Parkinson's disease.[22] Regarding its role in oncogenesis, there are contradictory reports in the literature whether SIRT2 is a tumor suppressor or promoter.[23−25] Down-regulation of SIRT2 reduced the cell proliferation in glioma cells,[26] HeLa cells,[27] and liver[28] and pancreatic carcinomas.[29] Inhibition of SIRT2 by selective inhibitors such as **30** (AGK-2, Chart 2) and a 10,11-dihydro-5*H*-dibenz[*b*,*f*]azepine derivative have been shown to induce apoptosis in C6 glioma cells[26] and MCF-7 breast cancer cells,[30] respectively. Other small-molecule

Received: June 19, 2014
Published: November 10, 2014

SIRT2 inhibitors have shown to reduce cancer proliferation via the increase in p53 acetylation in nonsmall-cell lung cancer cells (A549 and H1299).[31] Hence, SIRT2 has been considered to be an interesting target for cancer drug development.

Recently, we showed that trisubstituted 2-alkyl-chroman-4-ones can serve as selective SIRT2 inhibitors with IC_{50} values in the low micromolar range.[32] Two of the most potent inhibitors are shown in Chart 1.

Chart 1. SIRT2 Selective Inhibitors Based on the Chroman-4-one Scaffold

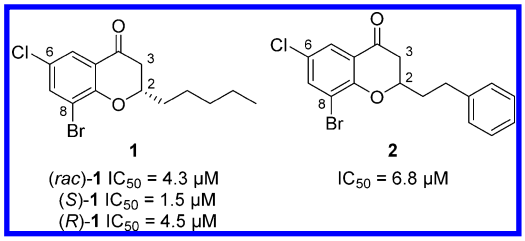

The structure–activity relationship (SAR) study revealed that electron-withdrawing groups on the aromatic ring of the bicycle, the carbonyl group, as well as an alkyl side chain in the 2-position are crucial for potent inhibitors. The SAR study also disclosed an exceptionally close relationship between the presence of all features mentioned above and the inhibitor potency as even minor modifications resulted in a severe loss of activity. Analysis of the individual enantiomers of **1** showed that the stereoisomers had only small differences in inhibitory activities, with (*S*)-**1** being slightly more potent (Chart 1).

However, the high lipophilicity of the published chroman-4-ones limits their use in more advanced biological in vivo and in vitro tests. Herein, we report chroman-4-one analogues based on lead compounds **1** and **2** as potential SIRT2 inhibitors with increased hydrophilicity. The hydrophilicity was increased by the introduction of heterofunctional groups such as terminal hydroxyl, carboxylic acid, ester, and amide moieties in the alkyl side chain in the 2-position of **1**. The phenyl ring in **2** was replaced with aromatic and aliphatic heterocycles. We also propose a binding mode of the chroman-4-ones based on a homology model of SIRT2. It showed to be consistent with the SAR data of the investigated compounds. Two potent inhibitors were chosen for further evaluation of their effect on cancer cells.

RESULTS AND DISCUSSION

Chemistry. The key reaction in the synthesis of the biologically evaluated compounds is the assembling of the chroman-4-one scaffold. The general synthetic strategy for the formation of chroman-4-ones **6a–i** is shown in Scheme 1 and involves the base-promoted aldol condensation between a substituted 2′-hydroxyacetophenone and an aldehyde, followed by an intramolecular *oxa*-Michael ring closure reaction. Commercially available alcohols (**3a**, **3d–g**) were used as precursors for the desired aldehydes, whereas alcohols **3b** and **3c** were synthesized via monoprotection of commercially available diols using NaH and TBDMSCl according to a procedure reported by McDougal et al.[33] The aldehydes (**4a–g**) were obtained via Swern or Dess–Martin oxidation and could be directly used in the next step without any further purification. For the ethylene glycol based aldehyde **4d**, the ordinary workup procedure involving addition of water and EtOAc had to be changed to a nonaqueous workup due to its high water solubility.

The chroman-4-ones **5a–c** and **6d–i** were synthesized in moderate to good yields by heating 2′-hydroxyacetophenones and the appropriate aldehydes in a microwave reactor for 1 h in ethanol using *N*,*N*-diisopropylamine (DIPA) as base. The TBDMS-protection group of **5a–c** was removed using electrophilic fluorine in a microwave-heated reaction,[34] providing the deprotected chroman-4-ones **6a–c** in 16–78% yield over three steps. Removal of the silyl protecting group of **5a** and **5b** with the more commonly used tetrabutylammonium fluoride (TBAF) in THF surprisingly yielded the ring opened products **7a** and **7b** (Scheme 2). No formation of the ring-opened byproduct was observed for **5c**. Treatment of the hydroxyl derivatives **6a** and **6b** with TBAF also resulted in the formation of ring opened products. The byproduct formation is likely to be attributed to the basicity of the fluoride ion in organic solvents. In separate experiments, it was however found

Scheme 1. General Synthetic Scheme towards the Substituted Chroman-4-ones 6a–i[a]

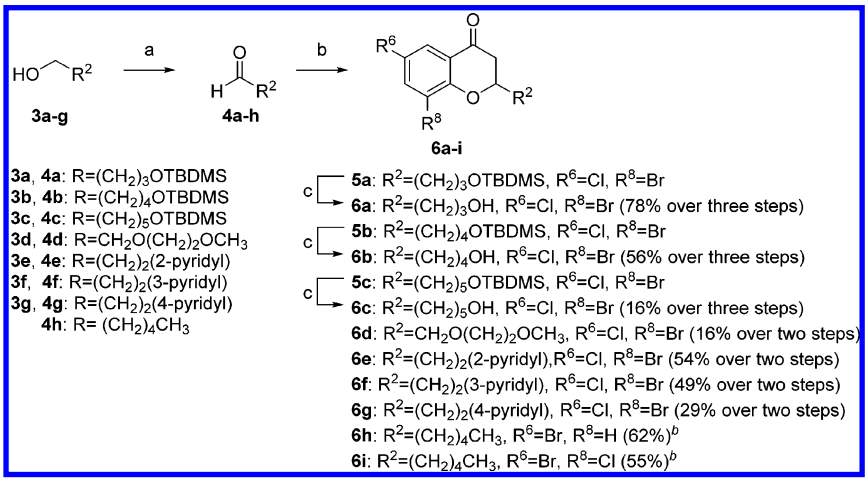

[a]Reagents and conditions: (a) (i) $(COCl)_2$, DMSO, THF, −78 °C, 30 min, (ii) appropriate alcohol, −78 °C, 30 min, (iii) Et_3N, −78 °C → room temp, 15 min, or Dess–Martin periodinane, CH_2Cl_2, room temp; (b) appropriate 2′-hydroxyacetophenone, DIPA, EtOH, MW, 170 °C, 1–2 h; (c) Selectfluor, MeOH, MW, 150 °C, 30 min. [b]Commercially available hexanal (**4h**) was used.

dx.doi.org/10.1021/jm500930h | J. Med. Chem. 2014, 57, 9870–9888

Scheme 2. Synthesis of Ring-Opened Derivatives Using TBAF[a]

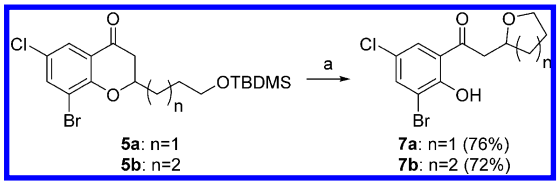

[a]Reagents and conditions: (a) TBAF, THF, room temp, overnight.

that the byproduct was not formed when triethylamine was used as base.

The ester analogues of **6a** and **6b** were prepared according to the synthetic route outlined in Scheme 3. δ-Valerolactone and

Scheme 3. Synthesis of Ester Derivatives of 2,6,8-Trisubstituted Chroman-4-ones[a]

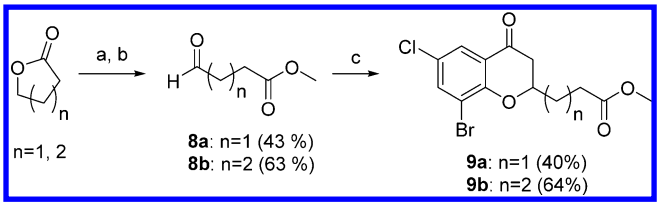

[a]Reagents and conditions: (a) Et_3N, MeOH, room temp, 18 h; (b) SO_3·pyridine, Et_3N, DMSO, room temp, 14 h, or (i) $(COCl)_2$, DMSO, THF, −78 °C, 30 min, (ii) appropriate alcohol, −78 °C, 30 min, (iii) Et_3N, −78 °C → room temp, 15 min; (c) 3′-bromo-5′-chloro-2′-hydroxyacetophenone, piperidine or DIPA, EtOH, 170 °C, 0.5−1 h.

γ-butyrolactone were ring-opened under basic conditions in MeOH. Alcohol oxidation provided aldehydes **8a** and **8b**, which were reacted with 3′-bromo-5′-chloro-2′-hydroxyacetophenone to afford **9a** and **9b** (Scheme 3).

As esters are prone to hydrolyze in vivo, we also wanted to test the corresponding carboxylic acid analogues for their SIRT2 inhibitory potency, as well as amide and oxadiazole analogues, which are hydrolytically more stable and also considered to be ester bioisosteres. Chroman-4-ones **9a−b** were believed to be good starting points to access the carboxylic acids as well as the different amide analogues. However, attempts to hydrolyze the ester functionality of **9b** under basic conditions (LiOH or Me_3SnOH) were unsuccessful. Neither were attempts to obtain the amide analogues by directly reacting 2-hydroxyacetophenones with δ-amido aldehydes, obtained by ring opening of δ-valerolactone with amines followed by oxidation of the obtained amido alcohols, successful.

Instead, oxidation of the primary alcohol of **6a** and **6b** by a Dess−Martin oxidation, followed by a Pinnick oxidation of the generated aldehydes, yielded the carboxylic acids **10a−b** (Scheme 4). The acids were then successfully coupled with different primary and secondary amines using *N*,*N*′-carbonyldiimidazole (CDI) as coupling reagent to provide amides **11a−e** in good to excellent yields (68−93%). Treatment of the CDI-activated acids **10a** or **10b** with acetamide oxime followed by heating provided the oxadiazoles **12a−b**.

To further explore the influence of the phenyl ring in lead compound **2** (Chart 1), pyridine rings (**6e−g**) and morpholine, piperidine, or piperazine moieties were planned to be incorporated. The latter chroman-4-ones were envisioned to

Scheme 4. Synthesis of Chroman-4-one-Based Carboxylic Acids 10a−b, Amide Analogues 11a−e, and Oxadiazoles 12a−b[a]

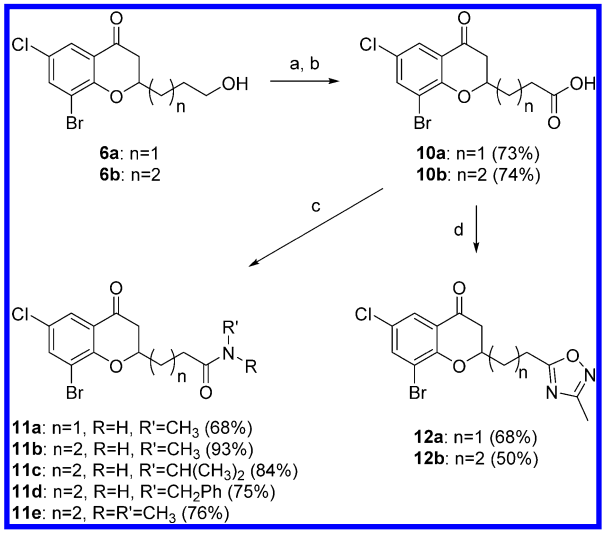

[a]Reagents and conditions: (a) Dess−Martin periodinane, CH_2Cl_2, room temp, 0.75−1 h; (b) $NaClO_2$, NaH_2PO_4·$2H_2O$, amylene, H_2O, THF, 0 °C → room temp; (c) (i) appropriate acid, CDI, CH_2Cl_2/DMF, 0 °C, 30 min, (ii) appropriate amine, 0 °C → room temp, 2−14 h; (d) (i) appropriate acid, CDI, MeCN/DMF, room temp, 30 min, (ii) acetamide oxime, 85 °C, 14−19 h.

be synthesized in analogy to the standard route outlined in Scheme 1 starting from commercially available alcohols as precursors (Scheme 5). However, neither Swern oxidation of 3-morpholinopropan-1-ol nor the use of other oxidizing agents such as Dess−Martin periodinane, TEMPO, TPAP, or CrO_3[35] resulted in the desired aldehyde **13**. Finally, **13** was obtained by conjugate addition of morpholine to acrolein (Scheme 5). Applying the standard procedure for approaching target compound **14a** was unsuccessful as well as attempts via preformation of the aldol intermediate using of lithium diisopropylamide (LDA). Attempts to approach the aliphatic heterocycles containing chroman-4-ones via a substitution reaction of a terminal hydroxyl group failed due to the unsuccessful reaction of the acetophenone and aldehyde **15**. None of the approaches resulted in the formation of the desired products.

Eventually, the prolongation of the spacer between the chroman-4-one scaffold and the heterocycle to propylene enabled the synthesis of related analogues of the phenethyl-substituted chroman-4-one **2**. The synthetic pathway toward the derivatives is outlined in Scheme 6. Compounds **17a** and **17b** were finally prepared from the mesylated chroman-4-one **16** via a microwave-assisted substitution reaction using morpholine and piperidine.

In addition to the above-described monocyclic heterofunctionalities, bicyclic groups were introduced to move the hydrogen-bonding groups further away from the scaffold. Two different ring systems were chosen, i.e., quinolin-6-yl and 3,4-dihydro-2(1*H*)-quinolinone-6-yl. The starting material 6-bromo-3,4-dihydro-2(1*H*)-quinolinone was prepared in analogy to the procedure reported by Tietze et al.[36] and Zaragoza et al.[37] Reaction of the bromo-substituted bicyclic systems with acetal-protected acrolein in a Heck reaction yielded **18a−b** (Scheme 7).[38] Catalytic hydrogenation and deprotection of the acetal under acidic conditions furnished the desired aldehyde

dx.doi.org/10.1021/jm500930h | J. Med. Chem. 2014, 57, 9870−9888

Scheme 5. Synthetic Attempts towards Chroman-4-ones 14a and 14b[a]

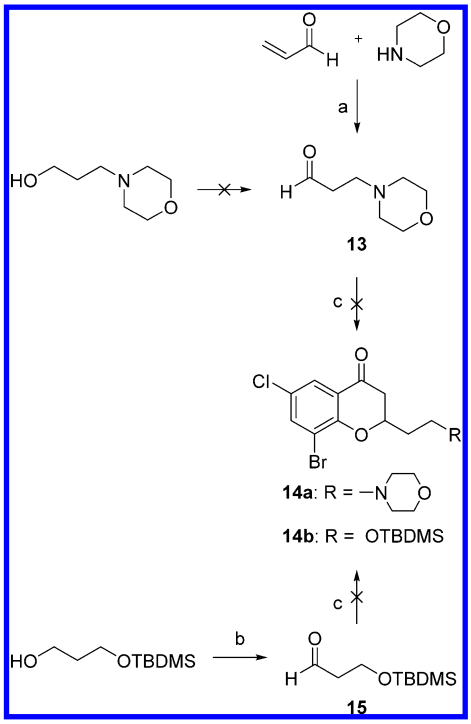

[a]Reagents and conditions: (a) MeCN, $MgSO_4$, room temp, overnight, 93% crude yield; (b) (i) $(COCl)_2$, DMSO, THF, −78 °C, 30 min, (ii) 3-(*tert*-butyldimethylsilyl)oxy-1-propanol, −78 °C, 30 min, (iii) Et_3N, −78 °C → room temp, 15 min, 97% crude yield; (c) 3′-bromo-5′-chloro-2′-hydroxyacetophenone, DIPA, EtOH, 170 °C, 1 h.

Scheme 6. Synthesis of Chroman-4-ones 17a−b with Aliphatic Heterocyclic Rings in the 2-Position[a]

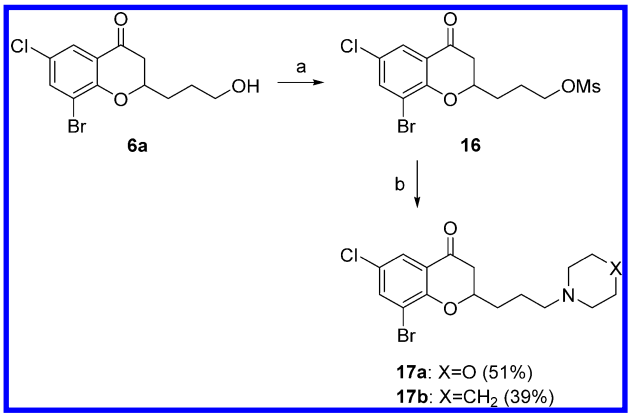

[a]Reagents and conditions: (a) MsCl, Et_3N, CH_2Cl_2, 0 °C → room temp; (b) morpholine or piperidine, THF, MW, 120−150 °C, 1 h.

19a (Scheme 7). Surprisingly, under the mild reducing conditions (H_2-balloon, 10% Pd/C, room temp) chosen to reduce the aliphatic double bond in **18b** also the quinoline moiety was reduced to yield the corresponding 1,2,3,4-tetrahydroquinoline. When Pd/C and 1,4-cyclohexadiene[39] was used as reducing agent, only reduction of the aliphatic double bond occurred, and after treatment with acid, the desired aldehyde (**19b**) was obtained. The aldehydes were then reacted under standard conditions with 3′-bromo-5′-chloro-2′-hydroxyacetophenone to yield **20a−b** in moderate yields.

Scheme 7. Synthesis of Chroman-4-ones Containing Bicyclic Heterofunctional Groups in the Side Chain in the R^2-Position[a]

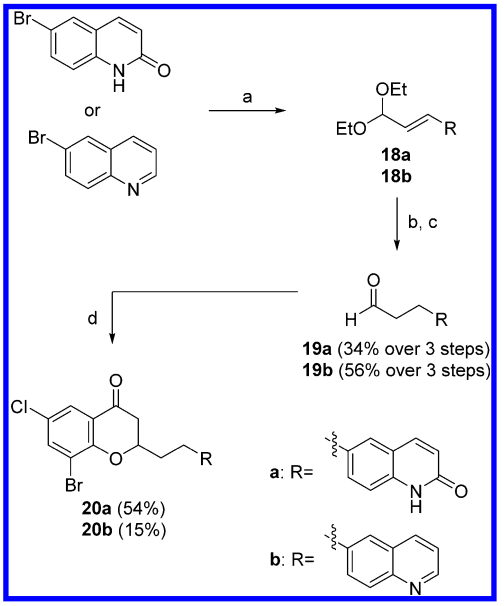

[a]Reagents and conditions: (a) appropriate aryl bromide, acrolein diethyl acetal, $Pd(OAc)_2$, KCl, K_2CO_3, TBAA, DMF, 90 °C, overnight; (b) H_2, 10% Pd/C, MeOH, room temp, 3 h or 1,4-cyclohexadiene, 10% Pd/C, EtOH, reflux, 4.5 h; (c) HCl (conc), acetone, reflux, 2−4 h; (d) 3′-bromo-5′-chloro-2′-hydroxyacetophenone, DIPA, EtOH, MW, 160−170 °C, 1.5−2 h.

The tetrasubstituted chromones **21−25** were synthesized as illustrated in Scheme 8. The monobrominated chroman-4-one **21** was obtained by reaction of **2** with $CuBr_2$. Treatment of **21** with NaN_3 in DMSO resulted in the formation of amine **22**,[40] which was acetylated with acetyl chloride in pyridine to form **23**. A SmI_2-mediated Reformatsky type reaction using tosyl cyanide as described earlier by Ankner et al. was successfully applied to introduce a nitrile moiety in the 3-position, and subsequent oxidation with DDQ in dioxane yielded 3-cyano-chromone **24**.[41] Further reduction of the nitrile group by means of DIBAL-H furnished enaminone **22** in 66% yield.

Molecular Modeling. *Mode of Action of Sirtuins and Inhibitor Binding.* Sirtuins contain a conserved enzymatic core comprising a Rossmann fold domain and a small domain containing a three-β-stranded zinc binding motif. The Rossmann fold contains six parallel β-strands forming a central β-sheet which is sandwiched between α-helices (number dependent on SIRT isoform) on either side of the β-sheet.[42,43] Between these domains the binding sites of NAD^+ and the acetylated peptide substrate are located. The NAD^+ binding site can be formally divided into the subpockets A (adenine binding site), B (ribose binding site), and C (nicotinamide binding site).[42] The binding of the peptide substrate and NAD^+ is proposed to take place in a sequential manner.[44] Binding of the peptide substrate induces the cleft between the two domains to close, and upon NAD^+ binding the cofactor binding loop gets ordered.[43,45] The presence of an acetyl lysine peptide promotes a strained, productive NAD^+ conformation, which is required for the deacetylation reaction to proceed. This conformation positions the nicotinamide moiety of NAD^+ in the C-pocket and brings the ribose ring in vicinity of the acetyl group in the peptide substrate.[42,43,46]

dx.doi.org/10.1021/jm500930h | J. Med. Chem. 2014, 57, 9870−9888

Scheme 8. Synthesis towards Tetrasubstituted Chromone Derivatives[a]

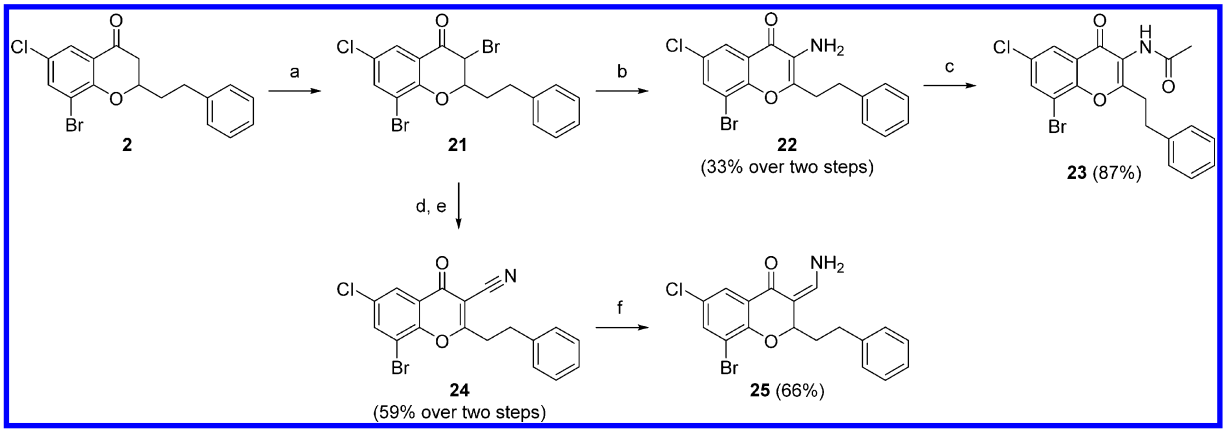

[a]Reagents and conditions. (a) $CuBr_2$, $CHCl_3$/EtOAc, 2 h, reflux; (b) NaN_3, DMSO, 70 min, room temp; (c) AcCl, pyridine, room temp, overnight; (d) SmI_2, KHMDS, TsCN, THF, −78 °C → room temp, *cis*:*trans* 29:71; (e) DDQ, dioxane, room temp, 12 h; (f) DIBAL-H, CH_2Cl_2, −78 °C, 3 h.

The C-pocket is the presumable binding site for potent small-molecular SIRT1/2 inhibitors (Chart 2) such as **30**,[22] thieno[3,2-*d*]pyrimidine-6-carboxamides (**31**),[47] 3-arylideneindolin-2-ones (**32**),[48] salermide (**33**),[49] cambinol (**34**),[50] and splitomicin analogues (**35**)[51] and **36**.[52] We therefore wanted to investigate whether this pocket could be a feasible binding site also for our compounds.

Chart 2. Structures of SIRT1/2 Inhibitors Known to Occupy the C-Pocket of the NAD$^+$-Binding Site and Our Chroman-4-one-Based Inhibitor 6f

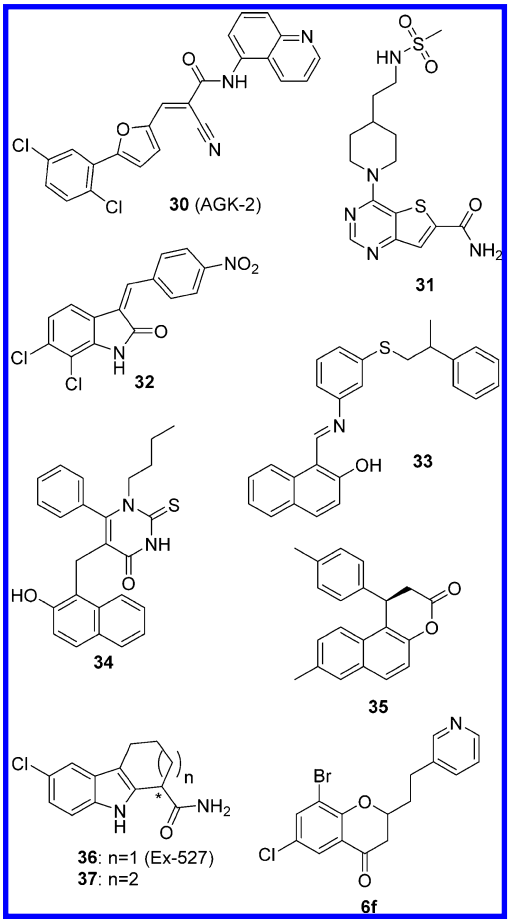

Homology Modeling of Human SIRT2. Four crystal structures of SIRT2 are currently available.[53−55] Two of these are apo-structures (PDB codes 1J8F and 3ZGO (3ZGO is a rerefined structure of the human SIRT2 apoenzyme 1J8F)),[53,54] lacking both peptide substrate and NAD$^+$ in their catalytic site. Their structures differ considerably compared to structures where peptide substrate and/or NAD$^+$ are bound. Another SIRT2 structure in complex with ADP-ribose (ADPr) was recently solved (3ZGV).[54] ADPr is similar to NAD$^+$ in structure; it binds in the NAD$^+$ binding cleft and thereby induces the conformational change which closes the active site crevice around ADPr in the Rossmann-fold domain. The fourth structure (4L3O) is a complex of SIRT2 with inhibitor S2iL5, which is a macrocycle binding from the outside into the peptide binding channel.[55] Because the structure with ADPr (3ZGV) lacks a bound inhibitor and includes ADPr instead of NAD$^+$ and the macrocycle in the latest solved structure (4L3O) largely differs from the small molecular chroman-4-ones, we decided to construct a homology model of SIRT2 based on a more suitable template.

Recently, crystal structures were published of both SIRT3 and Sir2Tm with (*S*)-**36** (Chart 2) present in the C-pocket.[52] Also SIRT1 binding (*S*)-**37** (Chart 2) has been crystallized.[56] The Sir2Tm structure (PDB code 4BV2) is a complex which includes NAD$^+$, (*S*)-**36**, and a peptide substrate, but as it has a rather low resolution (3.3 Å) it was considered not to be the most suitable template for homology modeling. The structures that are solved of SIRT3 with inhibitor (*S*)-**36** (PDB 4BV3) and SIRT1 with (*S*)-**37** (PDB 4I5I) bound in the C-pocket seemed suitable as the size and shape of these compounds are similar to the chroman-4-one-based inhibitors. Of the two structures considered, the SIRT3/NAD$^+$/(*S*)-**36** structure (PDB 4BV3) binds NAD$^+$ in a nonproductive mode, with the nicotinamide moiety rotated 180° relative to the C-pocket and instead positioned in the peptide binding channel. Like (*S*)-**36** and (*S*)-**37**, the chroman-4-ones do not appear to be peptide substrate competitive inhibitors (data not shown), therefore the SIRT1/NAD$^+$/(*S*)-**37** complex (PDB code 4I5I) was chosen as a template for homology modeling.[56] Models were constructed that included a lysine residue from a Sir2-p53 peptide−NAD$^+$ complex (2H4F)[46] together with NAD$^+$ and inhibitor (4I5I). The homology modeling was performed using the MOE software (v. 2012.10, Chemical Computing Group Inc.: Montreal).

dx.doi.org/10.1021/jm500930h | *J. Med. Chem.* 2014, 57, 9870−9888

A multiple sequence alignment was performed in ClustalW (v. 2.1)[57] using the template (SIRT1 human, 4I5I (Q96EB6)),[56] the main target (SIRT2 human, Q8IXJ6), and the human SIRT3 sequence (Q9NTG7). The alignment was fine-tuned to improve the final homology model (Figure S1, Supporting Information). A detailed description of the homology modeling procedure is given in the Supporting Information. The force field used in the homology modeling in this study was Amber12:EHF with R-Field solvation, as implemented in the MOE software.

During the construction of the homology model, inhibitor **6f** was positioned in the C-pocket close to the location of **37** in the SIRT1 structure in order to achieve more information regarding the inhibitor–enzyme interactions. NAD^+ was included in the modeling procedure with its geometry kept from the SIRT1 structure, i.e., in its nonproductive mode. The lysine residue from a Sir2-p53 peptide–NAD^+ complex (2H4F) was included,[46] as were five structural water molecules from the SIRT1 structure (4I5I) positioned within 5 Å from the inhibitor (W2, W5, W17, W74, and W78). The selected inhibitor-induced SIRT2 homology model showed good geometrical properties (see Ramanchandran plots in Figure S2 in the Supporting Information). In the resulting homology model the chroman-4-one scaffold of inhibitor **6f** is buried in a hydrophobic and well-defined binding pocket. The carbonyl oxygen of **6f** forms a hydrogen bonding interaction with a conserved water molecule W17 (Figure 1).[52,54,58] There is also a halogen bonding interaction from the chloride in the 6-position to the backbone carbonyl of His187 with a distance of 3.7 Å (Cl···O=) and an angle of 163.5° (C–Cl···O=), which is an acceptable geometry.[59] The bromide in the 8-position is located in a hydrophobic environment surrounded by Leu103, Phe119, Leu138, and Phe190. In addition, Phe96 is favorably positioned for π–π interaction with the halogen substituted aromatic ring of **6f**[60] although this interaction is not geometrically optimal as the rings are arranged in a shape which is in between a parallel displacement and a face-to-edge arrangement (r = 5.4 Å, θ = 53.7°, ω = 35.1°, for definition see Figure S3 in Supporting Information).[61] The 2-(pyridin-3-yl)ethyl moiety is positioned in a rather narrow hydrophobic channel (Figure 1), which is directed toward the surrounding solution. The pyridine nitrogen of **6f** forms a hydrogen bond with Gln142 but could instead easily interact with surrounding water molecules outside the enzyme (Figure 1a,b).

Evaluation of Inhibitory Activity. The inhibitory effect of the synthesized chroman-4-one/chromones on the activity of SIRT2 was evaluated using a fluorescence-based assay. Table 1 summarizes the results from the SIRT2 inhibition assay of the trisubstituted chroman-4-ones. For potent inhibitors, IC_{50} values were determined, and these compounds were also tested against SIRT1 and SIRT3. In general, highly potent inhibitors showed to be selective for the SIRT2 subtype (for SIRT1 and SIRT3 inhibition data, see Table S3 in Supporting Information).

The SIRT2 inhibition data for the tetrasubstituted chromones are summarized in Table 2. These chromone-based derivatives are moderately potent and selective SIRT2 inhibitors (Table 2).

Potent inhibitors were also tested for their inhibitory effect on members of other classes of HDACs. The test confirmed that the compounds exclusively inhibit the class III of lysine deacetylases (HDAC inhibition <10% at 200 μM, data not shown).

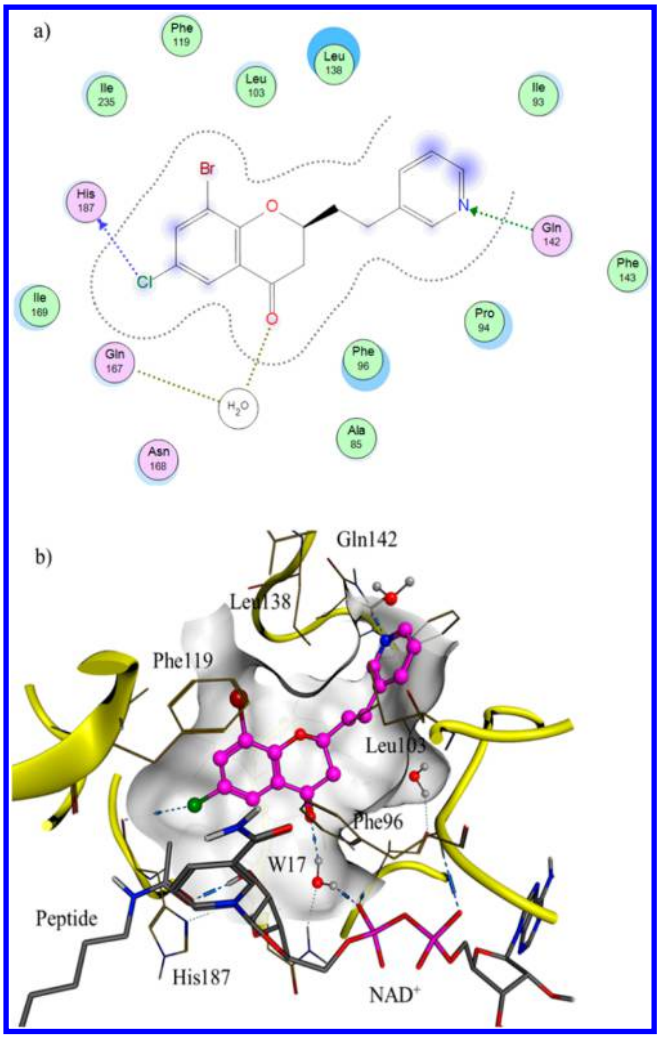

Figure 1. (a) Schematic view of the interactions between the chroman-4-one-based inhibitor **6f** and the human SIRT2 homology model. The carbonyl oxygen of **6f** interacts with a structural water molecule, which in turn interacts with a glutamine residue (Gln167) and with NAD^+. The bromide in the 8-position is buried in a hydrophobic environment (Leu103, Phe119, Leu138, and Phe190) and the chloride in the 6-position can form a halogen bonding interaction to the backbone carbonyl of His187. The substituent in the 2-position is stretched through a hydrophobic tunnel surrounded by Ile93, Pro94, Leu103, and Leu138, which ends in the aqueous environment at the surface of the enzyme, where the pyridyl nitrogen interacts with Gln142 via hydrogen bonding. (b) SIRT2 homology model with inhibitor **6f** (magenta) present in the C-pocket indicating the same interaction points as in (a). The carbonyl group of the acetylated substrate peptide interacts with a hydroxyl group in the ribose moiety of NAD^+.

Physicochemical properties of this new series of chroman-4-one-/chromone-based inhibitors were calculated (Table S4, Supporting Information). The results indicate that the structural modifications did lead to less lipophilic compounds with improved physicochemical properties. As illustrated in Table 3, the potent inhibitors of the new series have similar inhibitory activity as lead compounds **1** and **2**, however they exhibit more attractive physicochemical properties such as decreased clogP and clogD-values as well as a larger PSA (Table 3). Among the synthesized compounds, derivatives **6f** and **12a** were chosen for evaluation of a potential antiproliferative effect (see below Figure 3). Although the methyl ester **9b** is the most potent inhibitor and **9a** is as active

dx.doi.org/10.1021/jm500930h | J. Med. Chem. 2014, 57, 9870–9888

Table 1. Results from Evaluation of Trisubstituted Chroman-4-ones in a SIRT2 Inhibition Assay

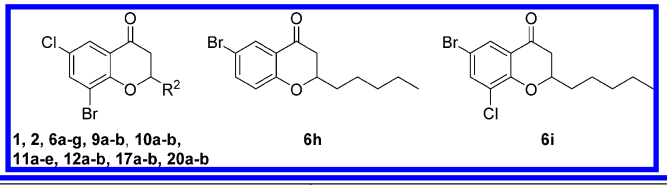

No.	R^2	Inhib (%)[a,b]	IC_{50} (μM)[c,d]	No.	R^2	Inhib (%)[a,b]	IC_{50} (μM)[c,d]
rac-1	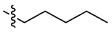	88 ± 0.9	4.3 (3.5–5.4)	10a	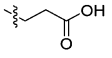	6.8 ± 1.5	n.d.
2	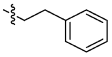	81 ± 0.7	6.8 (5.8–8.0)	10b	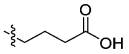	7.6 ± 1.6	n.d.
6a	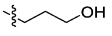	18 ± 1.1	n.d.	11a	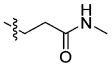	0.2 ± 4.8	n.d.
6b		52 ± 0.9	n.d.	11b	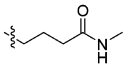	39 ± 0.9	n.d.
6c	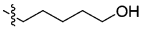	69 ± 0.5	n.d.	11c	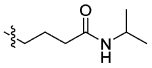	23 ± 1.8	n.d.
6d	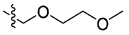	33 ± 2.0	n.d.	11d	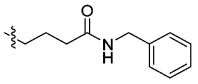	39 ± 0.9	n.d.
6e	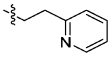	74 ± 0.5	n.d.	11e	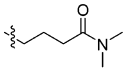	53 ± 1.4	n.d.
6f	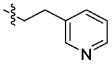	86 ± 1.9	3.7 (3.1–4.5)	12a	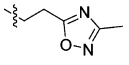	77 ± 0.8	12.2 (10.2–14.7)
6g	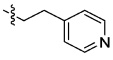	73 ± 1.8	n.d.	12b	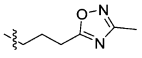	49 ± 1.2	n.d.
6h		69 ± 1.2	n.d.	17a	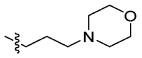	17 ± 10.7[e]	n.d.
6i		96 ± 2.8	1.8 (1.5–2.1)	17b	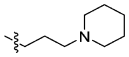	40 ± 2.8[e]	n.d.
9a	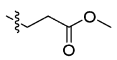	80 ± 4.4	9.6 (6.8–13.6)	20a	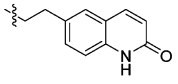	59 ± 1.1	n.d.
9b	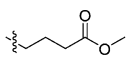	90 ± 0.5	2.0 (1.6–2.5)	20b	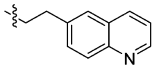	56 ± 1.1	n.d.

[a]SD, standard deviation (n = 3). [b]Inhibition at 200 μM inhibitor concentration. Suramin was used as reference compound in the assay. [c]IC_{50} (95% confidence interval). IC_{50} values were determined for compounds showing >80% inhibition of SIRT2 at 200 μM concentration or compounds evaluated in the cell proliferation assay. [d]n.d.= not determined. [e]The SIRTAinty assay was used for the determination.

as **12a**, the methyl ester group is prone to hydrolysis in the cell-based assay, yielding the biologically inactive carboxylic acids analogues **10a** and **10b**, therefore **9a** and **9b** were not further investigated.

dx.doi.org/10.1021/jm500930h | J. Med. Chem. 2014, 57, 9870–9888

Table 2. Results from Evaluation of the Tetrasubstituted Chromones in a SIRT2 Inhibition Assay

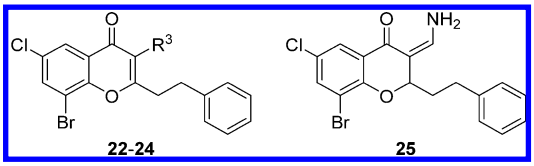

no.	R^3	inhib (%)[a,b]	IC_{50} (μM)[c,d]
22	NH_2	79 ± 1.5	nd
23	NHAc	81 ± 0.9	28.7 (21.4–38.5)
24	CN	50 ± 1.9	nd
25		76 ± 1.9	nd

[a]SD, standard deviation (n = 3). [b]Inhibition at 200 μM inhibitor concentration. [c]IC_{50} (95% confidence interval). IC_{50} value was determined for compounds showing >80% inhibition. [d]nd = not determined.

Table 3. Data of Calculated Physicochemical Properties of Lead Compounds 1 and 2 and of 6f, 9a–b, and 12a from the New Series

no.	IC_{50} (μM)	MW	ACDlogP	ACDlogD pH 7.4	PSA (Å^2)	HBD[a]	HBA[b]
1	4.3	331.6	5.60	5.60	27.4	0	2
2	6.8	365.7	5.57	5.57	27.4	0	2
6f	3.7	366.6	4.19	4.18	37.6	0	3
9a	9.6	347.6	3.36	3.36	54.4	0	4
9b	2.0	361.6	3.77	3.77	54.4	0	4
12a	12.2	371.6	3.69	3.69	61.0	0	5

[a]Number of hydrogen bond donors. [b]Number of hydrogen bond acceptors.

Structure–Activity Relationships. In this study, we have focused on chroman-4-ones/chromones with increased hydrophilicity. This was achieved by the introduction of aliphatic and aromatic mono/bicyclic moieties with hydrogen-bonding groups in the 2-position of the chroman-4-ones as well as the implementation of hydrogen bonding groups in the 3-position of the chromones. These changes were done to improve the inhibition of SIRT2 but also to obtain information about space limitations caused by the introduction of bulkier groups.

The substituent in the 2-position is crucial for SIRT2 inhibition because 6-bromochroman-4-one lacking a substituent in the 2-position does not show any inhibition (data not shown), while the corresponding analogue **6h**, which has a pentyl group in the 2-position, shows an inhibitory activity of 70% (Table 1). Replacement of the pentyl side chain in lead compound **1** with a more polar ethylene glycol side chain (**6d**) resulted in a significant decrease in activity (33% inhibition) as did the introduction of a terminal hydroxyl group (**6a**, 18% inhibition). However, by increasing the length of the linker between the OH-group and the scaffold (**6b** and **6c**), some activity could be retained (Table 1). Still, **6c** (67% inhibition) is less potent then the lead compound ((*rac*)-**1**, 88%). This indicates that highly polar side chains (**6d**) and hydrogen bond donating groups are not favorable with a chain length up to five atoms. This observation can be explained by the homology model, which shows that five out of seven amino acids surrounding this channel are hydrophobic (Ile93, Pro94, Leu103, Leu138, and Phe143, Figure 1a and Figure S1 in the Supporting Information). One of two hydrophilic amino acids (Asp170) is rotated away from the substituent in the 2-position while the other (Gln142) is directed toward the aqueous solution, which might explain the enhanced activity with increasing length of the spacer for alcohols **6a–c**. Replacement of the phenyl ring in **2** with a pyridyl moiety (**6e–g**) resulted in compounds with similar activity and improved solubility. The 3-pyridyl substituted chroman-4-one (**6f**) was with 86% inhibition most potent compared to the 2- and 4-pyridyl analogues **6e** and **6g**. Modeling results showed that the pyridyl moiety of **6f** has an optimal geometry to form a hydrogen bond with Gln142, which is located at the end of the hydrophobic channel toward the aqueous solution (Figure 1b). This hydrogen bonding interaction can also be observed for the ester functionality in **9a** and **9b**, the latter being one of the most potent inhibitors with an IC_{50} value of 2.0 μM. As earlier mentioned, esters are prone to hydrolysis under physiological conditions and therefore also the corresponding acids were investigated. However, the carboxylic acids **10a** and **10b** were completely inactive, which could be attributed to carboxylate formation at physiological pH. Negatively charged groups are unfavorable in the lipophilic and narrow channel accommodating the R^2-substituent. The replacement of the methyl ester in **9a–b** with a methyl amide (**11a** and **11b**) dramatically lowered the activity. Also replacement of the methyl amide with the bulkier *iso*-propyl (**11c**) or benzyl amides (**11d**) gave no increase in inhibitory potency. Only the dimethyl amide **11e** was slightly more potent, with 53% inhibition compared to 39% for the monomethyl amide. The secondary amides (**11a–d**) can act both as hydrogen bond accepting and donating group, and here it seems as the presence of an NH-group decreases the activity. However, all amide analogues are not as active as the methyl esters (**9a–b**). An explanation for this could be that an NH-group is less favorable in the lipophilic environment than the less hydrophilic single bonded oxygen of the ester. This statement was supported in docking studies[62,63] of **9b** and **11b**, where the *O*- and *N*-methyl groups are positioned in a small hydrophobic pocket rather than toward the aqueous solution (Figure 2). Thereby, the single-bonded oxygen in the ester and the NH-moiety in the amide are oriented toward the hydrophobic site, which makes the more polar amide

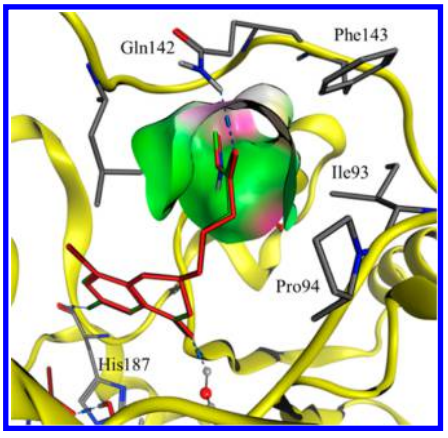

Figure 2. Docked chroman-4-one analogues **9b** (red) and **11b** (green) in the SIRT2 homology model. The green part of the surface is hydrophobic while the purple is hydrophilic. The carbonyl oxygens are forming hydrogen bonds with the glutamine residue Gln142, and the methyl groups are positioned in a small hydrophobic pocket. The polar hydrogen on the amide is pointing toward a hydrophobic region. Only the water molecule interacting with the carbonyl group in the chroman-4-ones (W17) is shown.

dx.doi.org/10.1021/jm500930h | J. Med. Chem. 2014, 57, 9870–9888

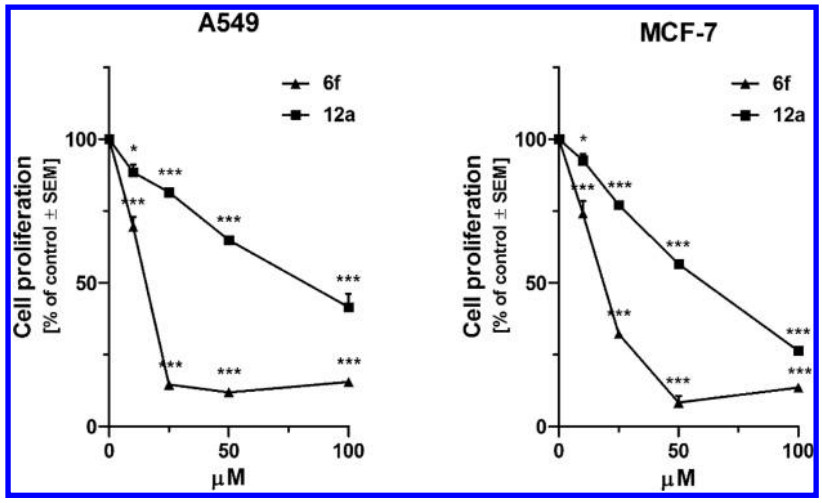

Figure 3. SIRT2 inhibitors reduce A549 (left) and MCF-7 (right) cancer cell proliferation. The cells were treated with 0−100 μM of **6f** and **12a**. Cell proliferation was determined by a sulforhodamine B assay. The results are shown as mean ± SEM of two to three independent experiments. The asterisks indicate significant differences (* $P < 0.05$, *** $P < 0.001$ when compared to controls).

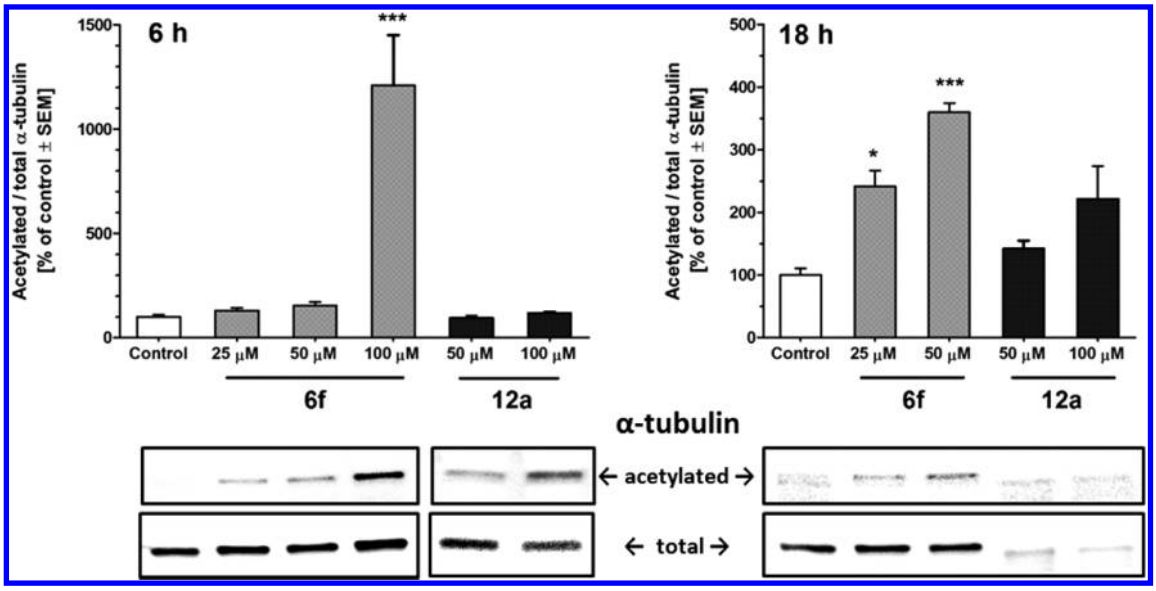

Figure 4. Effects of SIRT2 inhibitors on α-tubulin acetylation. MCF-7 cells were treated for 6 h (left panel) or 18 h (right panel) with 40 nM Trichostatin A plus indicated concentrations of **6f** or **12a**. The results are shown as mean ± SEM of three independent experiments. The asterisks indicate significant differences (* $P < 0.05$, *** $P < 0.001$ when compared to controls). The representative Western blots are shown below.

unfavorable compared to the ester. Compound **11e** is still less active than **9b**, which could be explained by the steric bulk of the dimethyl amide in the narrow tunnel.

The oxadiazole derivative with an ethylene linker (**12a**, IC_{50} = 12.2 μM) was equipotent to the corresponding methyl ester. Surprisingly, the bioisosteric replacement of the methyl ester moiety of **9b** with an oxadiazole group (**12b**) resulted in lower potency. Docking studies showed that **12a** can adopt a similar binding pose as the ester whereas the methyl group of the longer oxadiazole **12b** did not fit in the binding channel. The morpholine- and piperidine-substituted analogues **17a** and **17b** showed 17% and 40% inhibition, respectively. The morpholine and piperidine moieties are rather bulky, and the extended spacer places the groups further away from the scaffold and closer to the narrow part of the channel. Beside this, piperidine and morpholine are charged at pH 7.4, which seems unfavorable in the hydrophobic binding pocket. The chroman-4-one derivatives with the quinolinone and quinoline moieties (**20a** and **b**) were moderate inhibitors with 59% and 56% inhibition, respectively. These results are consistent with a previously published indolyl-substituted derivative,[32] which had 53% inhibitory activity. The rather narrow hydrophobic channel accommodating the side chain seems to be large enough to accommodate monocyclic ring systems rather than the large bicyclic moieties. Interestingly, the 6-bromo-8-chloro-chroman-4-one derivative **6i** (IC_{50} 1.8 μM) showed twice the activity of racemic **1** (IC_{50} 4.3 μM), which strengthens the hypothesis of a halogen bonding interaction between the halide in the 6-position and the backbone carbonyl. A bromide is a better halogen bonding group than chloride, and therefore **6i** was supposed to be more active than lead compound **1**.

The chromones (Table 2) with an additional substituent in the 3-position showed generally only moderate inhibitory activity (50−81%). The acetamide substituted phenethyl-chromone **23** was the best inhibitor, with 81% inhibition and an IC_{50} value of 29 μM. The introduction of the small

dx.doi.org/10.1021/jm500930h | J. Med. Chem. 2014, 57, 9870−9888

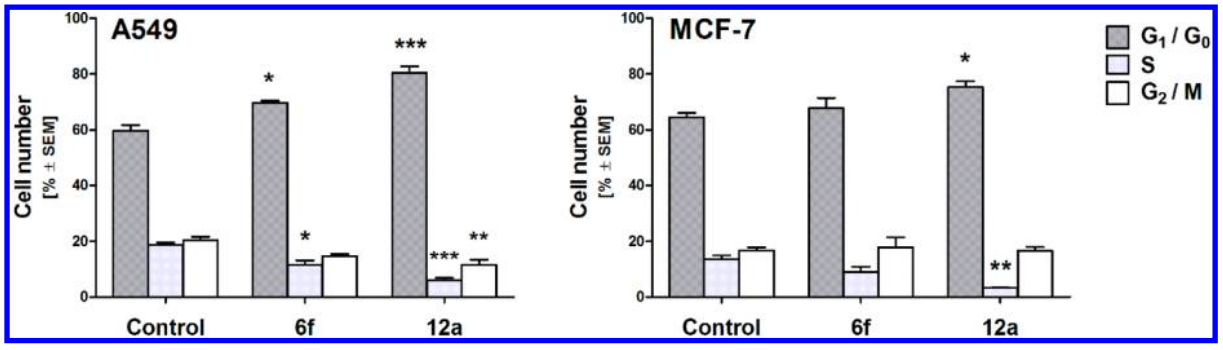

Figure 5. Effects of SIRT2 inhibitors on A549 (left) and MCF-7 (right) cell cycles. The cells were subjected to control treatment (0.5% DMSO) or treatment with **6f** (50 μM) or **12a** (100 μM) for 18 h. Flow cytometric analysis of DNA content was done after propidium iodide staining. Percentage of cells in each phase of the cell cycle (G_1/G_0, S, and G_2/M) is indicated. The results are shown as mean ± SEM of two to four independent experiments. The asterisks indicate significant differences (* $P < 0.05$, ** $P < 0.01$, *** $P < 0.001$ when compared to controls).

heterofunctional side chain on the flat ring system did not result in the desired increase in potency via additional hydrogen bonding interactions.

Evaluation of Antiproliferative Properties. We have previously shown that SIRT1/2/3 pan-inhibitors[64] with a well-documented mechanism of sirtuin inhibition[45,65] can cause antiproliferative effects in MCF-7 breast cancer and A549 lung cancer cell lines. Literature reveals that also SIRT2 inhibitors have been shown to have an antiproliferative effect in MCF-7 breast cancer cells[30,66] and A549 lung cancer cells.[31] We therefore wanted to study whether the novel compounds could achieve similar effects. Two potent inhibitors (**6f**, **12a**) with acceptable physicochemical profiles were chosen for testing in cancer cell proliferation assays. These two human cancer cell lines were exposed to increasing concentrations of **6f** and **12a**, and the cell proliferation was measured using a sulforhodamine B assay. Both compounds had a strong inhibitory effect on cancer cell growth (Figure 3). Compound **6f** showed a significant antiproliferative effect already at 10 μM concentration, and under microscopic evaluation there were no living cells visible after 48 h with higher concentrations (≥50 μM) of **6f** (data not shown).

SIRT2 is known to deacetylate α-tubulin.[67] To confirm the functionality of **6f** and **12a** as SIRT2 inhibitors in a cellular environment, MCF-7 cells were treated with these compounds and subjected to Western blot analysis of α-tubulin acetylation levels. After 6 h, treatment with 100 μM **6f** had produced a drastic increase in acetylated α-tubulin and lower concentrations of **6f** had weaker effects to the same direction (Figure 4). After 18 h, all cells treated with 100 μM **6f** had died and no sample could be obtained for Western blotting. Nevertheless, **6f** gave significant levels of inhibition of α-tubulin deacetylation at lower concentrations at this time point. Treatments with 50 and 100 μM of **12a** decreased total α-tubulin after 18 h. When compared to total α-tubulin, there was a clear, albeit nonsignificant trend toward increased α-tubulin acetylation in these samples.

Flow cytometric cell cycle analysis was performed in order to examine the basis for the antiproliferative effects of **6f** and **12a**. Treatment of MCF-7 or A549 cells for 18 h with 100 μM **12a** resulted in cell cycle arrest, as there was a significant increase in the fraction of cells in G_1/G_0 phase and a significant decrease in the fraction of cells in DNA synthesis phase (Figure 5). Furthermore, the fraction of A549 cells in G_2 phase decreased. Treatment with 50 μM **6f** also resulted in similar cell cycle arrest in A549 cells (significant) and MCF-7 cells (trend) (Figure 5). No apoptosis was observed in any of the samples (data not shown). The G_1/G_0 arrest is not necessarily resulting from increased acetylation of α-tubulin but may result from some other SIRT2-mediated event, and similar observations have been found in the literature.[31,68−70]

■ CONCLUSION

A series of chroman-4-ones carrying heterofunctional groups in the side chain in the 2-position together with four tetrasubstituted chromones were synthesized in good yields using efficient synthetic methods. Compared to the previously published chroman-4-ones, calculations of the physicochemical properties indicate that the new compounds show improved pharmacokinetic properties. Analogues carrying hydrogen bond accepting groups, e.g., pyridyl or ester moieties, were highly potent and selective SIRT2 inhibitors with low micromolar IC_{50} values. Two compounds (**6f** and **12a**) were chosen for investigation of their effects on cell proliferation in MCF-7 breast cancer and A549 lung cancer cells. Both compounds showed antiproliferative effects which correlate with their SIRT2 inhibition potency. SIRT2 is likely to be the target in the cancer cell lines, as we could show that the degree of acetylation of α-tubulin increased in a dose-dependent manner. A homology model of SIRT2 based on a SIRT1 crystal structure was built, and docking studies clarified the binding mode of the chroman-4-one-based inhibitors. The proposed binding mode of our compounds was similar to other reported SIRT inhibitors in that they occupy the nicotinamide binding site and prevent NAD^+ to bind in a catalytically active conformation. The docking studies contributed also to a deeper understanding of the SAR data. However, the reasons behind the isoform selectivity of the chroman-4-ones are still unclear but work is ongoing to get an understanding of the selectivity profile and to verify the binding mode.

■ EXPERIMENTAL SECTION

General. All reactions were carried out using magnetic stirring under ambient atmosphere if not otherwise noted. Room temperature corresponds to a temperature interval from 20 to 21 °C. All starting materials and reagents were obtained from commercial producers and were used without prior purification. Solvents were generally used as supplied by the manufacturer. Microwave reactions were carried out using a Biotage Initiator Sixty with fixed hold time modus in 0.5−2, 2−5 mL, or 10−20 mL capped microwave vials. All reactions were monitored by thin-layer chromatography (TLC) on silica plated aluminum sheets (Silica gel 60 F254, E. Merck). Spots were detected by UV light (254 or 365 nm). Purification by flash column

dx.doi.org/10.1021/jm500930h | J. Med. Chem. 2014, 57, 9870−9888

chromatography was performed using an automatic Biotage SP4 Flash + instrument. Prefabricated columns of two different cartridge sizes (surface area 500 m^2/g, porosity 60 Å, particle size 40−63 μm) were used. The NMR spectra were measured with a JEOL JNM-ECP 400 or a Varian 400-MR spectrometer. ^1H and ^{13}C NMR spectra were measured at 400 and 100 MHz, respectively. Chemical shifts are reported in ppm with the solvent residual peak as internal standard ($CDCl_3$ δ_H 7.26, δ_C 77.16; CD_3OD δ_H 3.31, δ_C 49.00; acetone-d_6 δ_H 2.05, δ_C 29.84; DMSO-d_6 δ_H 2.50, δ_C 39.52). All NMR experiments were measured at ambient temperature. Melting points were measured with a Mettler FP82 hot stage equipped with a FP80 temperature controller or Büchi Melting point B-545 and are uncorrected. Positive ion mass spectra (ESI-MS) were acquired with an LCQ quadrupole ion trap mass spectrometer (Finnigan LTQ) equipped with an electrospray ionization source or on a PerkinElmer API 150EX mass spectrometer. Combustion analyses for CHN were measured on a Thermo Quest CE Instruments EA 1110 CHNS-O elemental analyzer. High-resolution mass spectrometry (HRMS) analysis was performed on a Waters LCTp XE mass spectrometer with an Acquity UPLC BEH C18 (pH 10) or an Acquity UPLC CSH C18 (pH 3) column eluting with a gradient of 5−95% acetonitrile in water confirming ≥95% purity. Waters MassLynx 4.1 software was used for data analysis. Compounds **1**, **2**, and **20**−**23** have been synthesized according to procedures earlier reported by our group[32,40] and by Ankner et al.[41]

General Procedure for the Swern Oxidation to Obtain Aldehydes 4a−b,d−g. DMSO (3 equiv) was added dropwise to a solution of oxalyl chloride (1.2 equiv) in dry THF (0.1 M) at −78 °C under inert atmosphere, and the mixture was stirred for 30 min. The appropriate alcohol (1 equiv) in dry THF (0.5 M) was added dropwise to the reaction mixture, which was stirred for an additional 30 min at −78 °C. Et_3N (5 equiv) was added dropwise, and the mixture was stirred for 15 min before it was allowed to reach room temperature.

Workup Procedure A. Water and EtOAc were added, and the phases were separated. The aqueous phase was extracted with EtOAc, and the combined organic phases were washed with water and brine, dried over $MgSO_4$, and filtered, and the solvent was removed under reduced pressure.

Workup Procedure B. The precipitate was filtered off and rinsed thoroughly with EtOAc. The filtrate was concentrated under reduced pressure.

Aldehydes **4a−g** were directly used in the next step without further purification and full characterization.

*4-(tert-Butyldimethylsilyloxy)butanal (**4a**).* The aldehyde was synthesized according to the general procedure from 4-(*tert*-butyldimethylsilyl)oxy-1-butanol (1.01 g, 4.93 mmol), DMSO (1.0 mL, 14.1 mmol), oxalyl chloride (0.5 mL, 5.73 mmol), and Et_3N (3.4 mL, 24.4 mmol). Workup procedure A was used to afford **4a** (974 mg). The ^1H NMR spectrum of the crude product was in agreement with data reported in the literature.[71]

*5-(tert-Butyldimethylsilyloxy)pentanal (**4b**).* The aldehyde was synthesized according to the general procedure from 5-(*tert*-butyldimethylsilyl)oxy-1-pentanol **3b** (2.07 g, 9.48 mmol), DMSO (2.0 mL, 28.4 mmol), oxalyl chloride (1.0 mL, 11.4 mmol), and Et_3N (6.6 mL, 47.4 mmol). Workup procedure A was used to afford **4b** (2.00 g). The ^1H NMR spectrum of the crude product was in agreement with data reported in the literature.[72]

*6-(tert-Butyldimethylsilyloxy)hexanal (**4c**).* To a suspension of Dess−Martin periodinane (2.06 g, 4.86 mmol) in dry CH_2Cl_2 (10 mL) at 0 °C was dropwise added a solution of **3c** (0.75 g, 3.24 mmol) in dry CH_2Cl_2 (22 mL). The mixture was allowed to reach room temperature and was stirred for 1.5 h. The amount of solvent was reduced to half, the remaining mixture was diluted with Et_2O, and an aqueous solution of $Na_2S_2O_3/NaHCO_3$ was added. After 15 min, the phases were separated and the aqueous phase was extracted with EtOAc. The combined organic phases were washed with brine, dried over $MgSO_4$, filtered, and concentrated under reduced pressure. The ^1H NMR spectrum of the crude product was in agreement with data reported in the literature.[73]

*2-(2-Methoxyethoxy)acetaldehyde (**4d**).* The aldehyde was synthesized according to the general procedure from 2-(2-methoxyethoxy)ethanol (1.52 g, 12.6 mmol), DMSO (2.69 mL, 37.9 mmol), oxalyl chloride (1.32 mL, 15.2 mmol), and Et_3N (8.8 mL, 63.2 mmol). Workup procedure B was used to afford **4d** (2.83 mg).

*3-(Pyridin-2-yl)propanal (**4e**).* The aldehyde was synthesized according to the general procedure from 3-(pyridine-2-yl)propan-1-ol (71 mg, 0.52 mmol), DMSO (0.11 mL, 1.55 mmol), oxalyl chloride (0.50 mL, 0.62 mmol), and Et_3N (0.36 mL, 2.59 mmol). Workup procedure A was used to afford **4e** (70 mg). The ^1H NMR spectrum of crude product was in agreement with data reported in the literature.[74]

*3-(Pyridin-3-yl)propanal (**4f**).* The aldehyde was synthesized according to the general procedure from 3-(pyridine-3-yl)propan-1-ol (222 mg, 1.62 mmol), DMSO (0.34 mL, 4.85 mmol), oxalyl chloride (0.17 mL, 1.94 mmol), and Et_3N (1.13 mL, 8.10 mmol). Workup procedure A was used to afford **4f** (420 mg). The ^1H NMR spectrum of the crude product was in agreement with data reported in the literature.[74]

*3-(Pyridin-4-yl)propanal (**4g**).* The aldehyde was synthesized according to the general procedure from 3-(pyridine-4-yl)propan-1-ol (136 mg, 0.99 mmol), DMSO (0.21 mL, 2.97 mmol), oxalyl chloride (0.10 mL, 1.19 mmol), and Et_3N (0.69 mL, 4.96 mmol). Workup procedure A was used to afford **4g** (263 mg). The ^1H NMR spectrum of the crude product was in agreement with data reported in the literature.[74]

General Procedure for Synthesis of Chroman-4-ones 6a−i. The appropriate aldehyde (1.0 equiv) (commercially available or synthesized from the corresponding alcohol as mentioned above) and DIPA (1.1 equiv) were added to a 0.4 M solution of the appropriate 2′-hydroxyacetophenone (1.1 equiv) in EtOH. The mixture was heated by microwave irradiation at 170 °C for 1−2 h (fixed hold time, normal absorption), and the solvent was removed in vacuo. The residue was dissolved in EtOAc and washed with 10% NaOH (aq), 1 M HCl (aq), water, and finally with brine. The organic phase was dried over $MgSO_4$, filtered, and concentrated under reduced pressure. Purification by flash column chromatography gave chroman-4-ones **6d−i**. For the synthesis of **6a−c**, the corresponding TBDMS-protected chroman-4-ones **5a−c** were dissolved in MeOH (0.1 M), Selectfluor (0.2 equiv) was added, and the mixture was heated by microwave irradiation to 150 °C for 30 min. The mixture was concentrated and purified by flash column chromatography to give chroman-4-ones **6a−c**.

*8-Bromo-6-chloro-2-(3-hydroxypropyl)chroman-4-one (**6a**).* The compound was synthesized according to the general procedure from **4a** (crude, 974 mg), 3′-bromo-5′-chloro-2′-hydroxyacetophenone (1.28 g, 5.13 mmol), and DIPA (1 mL, 7.1 mmol) to give **5a** (2.00 g). An aliquot (460 mg, 1.06 mmol) was further reacted with Selectfluor (77 mg, 0.22 mmol). Flash column chromatography was performed using EtOAc/heptane (2:8 → 6:4) as eluent to afford **6a** (280 mg, 78% over three steps) as a white solid; mp 88−89 °C. ^1H NMR ($CDCl_3$) δ 7.78 (d, J = 2.5 Hz, 1H), 7.68 (d, J = 2.5 Hz, 1H), 4.64−4.48 (m, 1H), 3.83−3.70 (m, 2H), 2.79−2.66 (m, 2H), 2.10−1.75 (m, 4H). ^{13}C NMR ($CDCl_3$) δ 190.5, 156.6, 138.5, 127.1, 125.9, 122.4, 112.8, 79.0, 62.2, 42.6, 31.3, 28.3. Anal. ($C_{12}H_{12}BrClO_3$) C, H, N.

*8-Bromo-6-chloro-2-(4-hydroxybutyl)chroman-4-one (**6b**).* The compound was synthesized according to the general procedure from **4b** (crude, 2.00 g), 3′-bromo-5′-chloro-2′-hydroxy-acetophenone (2.65 g, 10.6 mmol), and DIPA (1.95 mL, 13.8 mmol). The obtained chroman-4-one **5b** (3.04 g) was directly reacted with Selectfluor (480 mg, 1.35 mmol). Flash column chromatography was performed using EtOAc/heptane (2:8 → 6:4) as eluent to afford **6b** (1.78 g, 56% over three steps) as a white solid; mp 94−96 °C. ^1H NMR ($CDCl_3$) δ 7.80 (d, J = 2.6 Hz, 1H), 7.70 (d, J = 2.6 Hz, 1H), 4.57−4.48 (m, 1H), 3.71 (t, J = 5.9 Hz, 2H), 2.79−2.66 (m, 2H), 2.05−1.92 (m, 1H), 1.84−1.50 (m, 5H). ^{13}C NMR ($CDCl_3$) 190.6, 156.7, 138.6, 127.1, 125.9, 122.5, 112.9, 79.0, 62.7, 42.5, 34.5, 32.3, 21.6. Anal. ($C_{13}H_{14}BrClO_3$) C, H, N.

*8-Bromo-6-chloro-2-(5-hydroxypentyl)chroman-4-one (**6c**).* The compound was synthesized according to the general procedure from **4c** (crude, 678 mg), 3′-bromo-5′-chloro-2′-hydroxyacetophenone (954 mg, 3.8 mmol), and DIPA (0.45 mL, 3.24 mmol). The obtained

dx.doi.org/10.1021/jm500930h | J. Med. Chem. 2014, 57, 9870−9888

chroman-4-one **5c** (805 mg) was further reacted with Selectfluor (123 mg, 0.35 mmol). Flash column chromatography was performed using EtOAc/heptane (4:6 → 6:4) as eluent to afford **6c** (186 mg, 16% over three steps) as a white solid; mp 110−112 °C. ^{1}H NMR ($CDCl_3$) δ 7.80 (d, J = 2.5 Hz, 1H), 7.70 (d, J = 2.6 Hz, 1H), 4.57−4.47 (m, 1H), 3.68 (t, J = 6.5 Hz, 2H), 2.79−2.65 (m, 2H), 2.03−1.90 (m, 1H), 1.81−1.41 (m, 7H). ^{13}C NMR ($CDCl_3$) δ 190.7, 156.8, 138.5, 127.0, 125.9, 122.5, 112.9, 79.0, 62.9, 42.6, 34.7, 32.7, 25.6, 25.0. Anal. ($C_{14}H_{16}BrClO_3$) C, H, N.

8-Bromo-6-chloro-2-((2-methoxyethoxy)methyl)chroman-4-one (6d). The compound was synthesized according to the general procedure from **4d** (crude, 50 mg), 3′-bromo-5′-chloro-2′-hydroxyacetophenone (106 mg, 0.42 mmol), and DIPA (86 μL, 0.85 mmol). Flash column chromatography was performed using EtOAc/heptane (3:7) as eluent to afford **6d** (24 mg, 16% over two steps) as an off-white solid; mp 61−63 °C. ^{1}H NMR ($CDCl_3$) δ 7.79 (d, J = 2.6 Hz, 1H), 7.69 (d, J = 2.6 Hz, 1H), 4.74−4.64 (m, 1H), 3.94−3.72 (m, 4H), 3.56 (t, J = 4.6 Hz, 2H), 3.37 (s, 3H), 2.91 (dd, J = 17.1, 12.4 Hz, 1H), 2.76 (dd, J = 17.1, 3.3 Hz, 1H). ^{13}C NMR ($CDCl_3$) δ 190.2, 156.5, 138.5, 127.2, 125.8, 122.4, 112.7, 78.3, 72.4, 72.1, 71.6, 59.2, 39.0. Anal. ($C_{13}H_{14}BrClO_4$) C, H, N.

8-Bromo-6-chloro-2-(2-(pyridine-2-yl)ethyl)chroman-4-one (6e). The compound was synthesized according to the general procedure from **4e** (crude, 70 mg), 3′-bromo-5′-chloro-2′-hydroxyacetophenone (130 mg, 0.53 mmol), and DIPA (0.1 mL, 0.71 mmol). Flash column chromatography was performed using EtOAc/heptane (2:8 → 55:45) as eluent to afford **6e** (102 mg, 54% over two steps) as a gray−black solid; mp 68−70 °C. ^{1}H NMR ($CDCl_3$) δ 8.54 (ddd, J = 4.9, 1.9, 0.9 Hz, 1H), 7.79 (d, J = 2.5 Hz, 1H), 7.71 (d, J = 2.6 Hz, 1H), 7.60 (ddd, J = 7.8, 7.5, 1.9 Hz, 1H), 7.24 (ddd, J = 7.8, 1.1, 0.9 Hz, 1H), 7.13 (ddd, J = 7.5, 4.9, 1.1 Hz, 1H), 4.57−4.44 (m, 1H), 3.20−3.01 (m, 2H), 2.81−2.69 (m, 2H), 2.42−2.20 (m, 2H). ^{13}C NMR ($CDCl_3$) δ 190.5, 160.3, 156.6, 149.6, 138.5, 136.7, 127.1, 125.9, 123.4, 122.5, 121.6, 112.9, 78.2, 42.6, 34.2, 33.5. Anal. ($C_{16}H_{13}BrClNO_2$) C, H, N.

8-Bromo-6-chloro-2-(2-(pyridin-3-yl)ethyl)chroman-4-one (6f). The compound was synthesized according to the general procedure from **4f** (crude, 420 mg), 3′-bromo-5′-chloro-2′-hydroxyacetophenone (445 mg, 1.78 mmol), and DIPA (0.34 mL, 2.41 mmol). Flash column chromatography was performed using EtOAc/heptane (20:80 → 55:45) as eluent to afford **6f** (289 mg, 49% over two steps) as a yellow solid; mp 81−82 °C. ^{1}H NMR ($CDCl_3$) δ 8.54 (d, J = 2.2 Hz, 1H), 8.47 (dd, J = 4.9, 1.6 Hz, 1H), 7.80 (d, J = 2.6 Hz, 1H), 7.73 (d, J = 2.5 Hz, 1H), 7.58 (dt, J = 7.8, 1.9 Hz, 1H), 7.24 (ddd, J = 7.8, 4.8, 0.8 Hz, 1H), 4.49−4.37 (m, 1H), 3.08−2.86 (m, 2H), 2.80−2.65 (m, 2H), 2.36−2.22 (m, 1H), 2.06−1.93 (m, 1H). ^{13}C NMR ($CDCl_3$) δ 190.1, 156.4, 150.2, 148.1, 138.7, 136.2, 135.9, 127.4, 126.0, 123.6, 122.5, 112.9, 77.3, 42.5, 36.1, 28.4. Anal. ($C_{16}H_{13}BrClNO_2$) C, H, N.

8-Bromo-6-chloro-2-(2-(pyridin-4-yl)ethyl)chroman-4-one (6g). The compound was synthesized according to the general procedure from an aliquot of **4g** (crude, 134 mg), 3′-bromo-5′-chloro-2′-hydroxyacetophenone (247 mg, 0.99 mmol), and DIPA (0.15 mL, 1.06 mmol). Flash column chromatography was performed using EtOAc/heptane (3:7 → 100% EtOAc) as eluent to afford **6g** (200 mg, 29% over two steps) as an off-white solid; mp 121−123 °C. ^{1}H NMR ($CDCl_3$) δ 8.53 (app d, 2H), 7.81 (d, J = 2.6 Hz, 1H), 7.74 (d, J = 2.6 Hz, 1H), 7.20 (app d, 2H), 4.49−4.38 (m, 1H), 3.07−2.87 (m, 2H), 2.81−2.69 (m, 2H), 2.36−2.23 (m, 1H), 2.08−1.95 (m, 1H). ^{13}C NMR ($CDCl_3$) δ 190.0, 156.4, 150.1, 149.6, 138.7, 127.4, 126.0, 124.1, 122.5, 112.8, 77.4, 42.5, 35.3, 30.6. Anal. ($C_{16}H_{13}BrClNO_2$) C, H, N.

6-Bromo-2-pentylchroman-4-one (6h). The compound was synthesized according to the general procedure from 5′-bromo-2′-hydroxyacetophenone (504 mg, 2.34 mmol), hexanal (0.31 mL, 2.58 mmol), and DIPA (0.37 mL, 2.63 mmol). Flash column chromatography was performed using toluene/heptane (1:1) as eluent to afford **6h** (433 mg, 62%) as a white solid; mp 42−44 °C. ^{1}H NMR ($CDCl_3$) δ 7.97 (d, J = 2.5 Hz, 1H), 7.53 (dd, J = 8.8, 2.5 Hz, 1H), 6.88 (d, J = 8.8 Hz, 1H), 4.47−4.37 (m, 1H), 2.74−2.60 (m, 2H), 1.93−1.81 (m, 1H), 1.75−1.64 (m, 1H), 1.60−1.25 (m, 6H), 0.95−0.87 (m, 3H). ^{13}C NMR ($CDCl_3$) δ 191.5, 160.7, 138.7, 129.5, 122.4, 120.2, 113.9, 78.3, 42.7, 34.9, 31.7, 24.7, 22.7, 14.1. Anal. ($C_{14}H_{17}BrO_2$) C, H, N.

6-Bromo-8-chloro-2-pentylchroman-4-one (6i). The compound was synthesized according to the general procedure from 5′-bromo-3′-chloro-2′-hydroxyacetophenone (498 mg, 2.00 mmol), hexanal (0.24 mL, 2.00 mmol), and DIPA (0.34 mL, 2.39 mmol). Flash column chromatography was performed using EtOAc/heptane (5:95) as eluent to afford **6i** (364 mg, 55%) as a white solid; mp 75−77 °C. ^{1}H NMR ($CDCl_3$) δ 7.90 (d, J = 2.4 Hz, 1H), 7.67 (d, J = 2.4 Hz, 1H), 4.56−4.46 (m, 1H), 2.79−2.65 (m, 2H), 2.01−1.88 (m, 1H), 1.79−1.67 (m, 1H), 1.67−1.29 (m, 6H), 0.95−0.85 (m, 3H).^{13}C NMR ($CDCl_3$) δ 190.6, 156.4, 138.2, 128.2, 124.5, 123.2, 113.2, 79.2, 42.6, 34.7, 31.6, 24.7, 22.6, 14.1. Anal. Calcd for $C_{14}H_{16}BrClO_2$: C, 50.70; H, 4.86. Found: C, 51.42; H, 4.86.

1-(3-Bromo-5-chloro-2-hydroxyphenyl)-2-(tetrahydrofuran-2-yl)ethanone (7a). A solution of TBAF in THF (1 M, 0.18 mL, 0.18 mmol) was added to a stirred solution of **5a** (53 mg, 0.12 mmol) in dry THF (11 mL), the reaction mixture was stirred at room temperature overnight. The mixture was concentrated under reduced pressure, and the crude product was purified by flash column chromatography using EtOAc/heptane (1:9) as eluent to afford **7a** (30 mg, 76%) as a pale-yellow oil. ^{1}H NMR ($CDCl_3$) δ 12.85 (s, 1H), 7.72 (s, 2H), 4.43−4.34 (m, 1H), 3.93−3.85 (m, 1H), 3.80−3.72 (m, 1H), 3.32 (dd, J = 16.1, 7.0 Hz, 1H), 3.05 (dd, J = 16.1, 5.4 Hz, 1H), 2.25−2.12 (m, 1H), 2.00−1.88 (m, 2H), 1.65−1.52 (m, 1H). ^{13}C NMR ($CDCl_3$) δ 203.8, 157.9, 139.0, 129.1, 124.0, 120.6, 113.1, 75.0, 68.2, 44.6, 31.8, 25.7.

1-(3-Bromo-5-chloro-2-hydroxyphenyl)-2-(tetrahydropyran-2-yl)ethanone (7b). A solution of TBAF in THF (1 M, 1.3 mL, 1.32 mmol) was added to a stirred solution of **5b** (197 mg, 0.44 mmol) in dry THF (2 mL), and the reaction mixture was stirred at room temperature for 17 h. The mixture was concentrated under reduced pressure, and the crude product was purified by flash chromatography using EtOAc/heptane (8:92) as eluent to afford **7b** (106 mg, 72%) as a yellow oil. ^{1}H NMR ($CDCl_3$) δ 12.90 (s, 1H), 7.74 (d, J = 2.5 Hz, 1H), 7.72 (d, J = 2.5 Hz, 1H), 3.97−3.83 (m, 2H), 3.50−3.37 (m, 1H), 3.26 (dd, J = 15.7, 7.7 Hz, 1H), 2.88 (dd, J = 15.7, 4.6 Hz, 1H), 1.94−1.81 (m, 1H), 1.75−1.29 (m, 5H). ^{13}C NMR ($CDCl_3$) δ 203.9, 157.9, 139.0, 129.3, 123.9, 120.9, 113.0, 74.2, 68.8, 45.2, 32.0, 25.8, 23.4.

Methyl 4-Oxobutanoate (8a). Et_3N (0.24 mL, 1.73 mmol) was added to a solution of γ-butyrolactone (0.40 mL, 5.20 mmol) in MeOH (5 mL). The mixture was stirred overnight at room temperature. Toluene was added, and the solvent was removed under reduced pressure to give the crude methyl 4-hydroxybutanoate as a colorless liquid. DMSO (0.74 mL, 10.4 mmol) was added dropwise to a solution of oxalyl chloride (0.36 mL, 4.16 mmol) in dry THF (21 mL) at −78 °C under inert atmosphere, and the mixture stirred for 30 min. Methyl 4-hydroxybutanoate (410 mg, 3.47 mmol) in dry THF (7 mL) was added dropwise to the reaction mixture which was stirred for an additional 30 min at −78 °C. Et_3N (2.42 mL, 17.3 mmol) was added dropwise, and the mixture was stirred for 15 min and was then allowed to reach room temperature. Water and EtOAc were added, and the phases were separated. The aqueous phase was extracted with EtOAc, and the combined organic phases were washed with water and brine, dried over $MgSO_4$, and filtered, and the solvent was removed under reduced pressure to give **8a** (293 mg, 43% over two steps). The crude product was sufficiently pure to be used in the next step without further purification. The ^{1}H NMR spectrum of crude product was in agreement with data reported in the literature.[75]

Methyl 5-Hydroxypentanoate (8b). Et_3N (2.0 mL, 14 mmol) was added to a solution of δ-valerolactone (4.2 g, 42 mmol) in MeOH (40 mL). The mixture was stirred for 18 h at room temperature. Toluene was added, and the solvent was removed under reduced pressure. A part of the crude alcohol (2.7 g, 20 mmol) and Et_3N (8.2 mL, 59 mmol) were dissolved in dry DMSO (40 mL) under inert atmosphere. A solution of SO_3·pyridine (9.3 g, 59 mmol) in DMSO (30 mL) was added dropwise, and the mixture was stirred for 14 h at room temperature. The mixture was poured on brine (400 mL) and ice (100 mL), and the product was extracted with CH_2Cl_2 and EtOAc. The combined organic phases were dried over Na_2SO_4, filtered, and concentrated under reduced pressure. Purification by flash chromatog-

dx.doi.org/10.1021/jm500930h | J. Med. Chem. 2014, 57, 9870−9888

raphy using EtOAc/hexane (2:8) gave **8b** (1.68 g, 63% over two steps). The ^{1}H NMR spectrum of crude product was in agreement with data reported in the literature.[76]

Methyl 3-(8-Bromo-6-chloro-4-oxochroman-2-yl)-propanoate (9a). 3′-Bromo-5′-chloro-2′-hydroxyacetophenone (591 mg, 2.37 mmol) was dissolved in EtOH (10 mL), DIPA (0.36 mL, 2.58 mmol) and **8a** (250 mg, 2.15 mmol) were added to a microwave vial, and the mix was heated in the microwave to 170 °C for 1 h. The solvent was removed, and the residue was redissolved in EtOAc. The organic phase was washed with 0.1 M HCl (aq), 1% and 10% NaOH (aq), water, and brine. The organic phase was dried over $MgSO_4$ and filtered, and the solvent was removed under reduced pressure. Purification by flash chromatography using EtOAc:pentane (1:4) gave **9a** (300 mg, 40%) as an off-white solid; mp 102−104 °C. ^{1}H NMR ($CDCl_3$) δ 7.81 (d, J = 2.3 Hz, 1H), 7.71 (d, J = 2.3 Hz, 1H), 4.65−4.50 (m, 1H), 3.72 (s, 3H), 2.89−2.53 (m, 4H), 2.30−2.01 (m, 2H). ^{13}C NMR ($CDCl_3$) δ 190.1, 173.2, 156.4, 138.6, 127.3, 126.0, 122.5, 112.9, 77.9, 52.0, 42.5, 29.9, 29.5. Anal. ($C_{13}H_{12}BrClO_4$) C, H, N.

Methyl 4-(8-Bromo-6-chloro-4-oxochroman-2-yl)butanoate (9b). 3′-Bromo-5′-chloro-2′-hydroxyacetophenone (242 mg, 0.97 mmol), **8b** (139 mg, 1.07 mmol), and piperidine (0.01 mL, 0.97 mmol) were added to a microwave vial followed by EtOH (2 mL). The mixture was heated by microwave irradiation to 170 °C for 30 min. The solvent was removed under reduced pressure. Purification by flash chromatography using EtOAc/hexane (12:88 and 2:8) gave **9b** (225 mg, 64%) as a yellow solid; mp 64−66 °C. ^{1}H NMR (CD_3OD) δ 7.82 (d, J = 2.5 Hz, 1H), 7.75 (d, J = 2.6 Hz, 1H), 4.65−4.55 (m, 1H), 3.67 (s, 3H), 2.85−2.69 (m, 2H), 2.47 (t, J = 7.0 Hz, 2H), 2.07−1.73 (m, 4H). ^{13}C NMR (CD_3OD) δ 192.1, 175.5, 158.1, 139.2, 127.7, 126.4, 123.8, 113.8, 80.3, 52.0, 43.1, 34.9, 34.3, 21.8. Anal. ($C_{14}H_{14}BrClO_4$) C, H, N.

3-(8-Bromo-6-chloro-4-oxo-chroman-2-yl)propanoic acid (10a). To a solution of **6a** (378 mg, 1.18 mmol) in dry CH_2Cl_2 (15 mL) Dess−Martin periodinane (785 mg, 1.80 mmol) was added. The mixture was stirred for 1 h at room temperature. The reaction was quenched by the addition of 10% $Na_2S_2O_3$/$NaHCO_3$ (aq). After 5 min, the mix was diluted with CH_2Cl_2 and H_2O and the aqueous phase was extracted with CH_2Cl_2. The combined organic phases were washed with brine, dried over $MgSO_4$, filtered, and concentrated under reduced pressure. The crude aldehyde (387 mg) was dissolved in THF (30 mL) and cooled to 0 °C. Amylene (1.25 mL, 11.8 mmol) was added, and $NaClO_2$ (321 mg, 3.55 mmol) and $NaH_2PO_4{\cdot}2H_2O$ (371 mg, 2.37 mmol) dissolved in H_2O (14 mL) were added dropwise. The ice bath was removed, and the mixture was stirred for 1 h. The reaction was quenched by the addition of a mixture of 1 M HCl and brine (1:1) and EtOAc. After 5 min of stirring, the phases were separated and the aqueous phase was extracted with EtOAc. The combined organic phases were washed with 1 M HCl/brine mix. The organic phase was extracted with 0.1 M NaOH (aq). The basic aqueous phase was acidified with 1 M HCl, and the acidic aqueous phase was extracted with EtOAc. The combined organic phases were finally washed with brine, dried over $MgSO_4$, filtered, and concentrated under reduced pressure. Flash column chromatography was performed using EtOAc/heptane (3:7) with 1% AcOH as eluent to afford **10a** (290 mg, 73% over two steps) as a white solid; mp 177−179 °C. ^{1}H NMR (CD_3OD) δ 7.84 (d, J = 2.6 Hz, 1H), 7.76 (d, J = 2.6 Hz, 1H), 4.70−4.58 (m, 1H), 2.90−2.54 (m, 4H), 2.21−2.03 (m, 2H). ^{13}C NMR (CD_3OD) δ 191.8, 176.4, 157.9, 139.2, 127.8, 126.4, 123.7, 113.9, 79.6, 43.0, 30.9, 30.4. Anal. ($C_{12}H_{10}BrClO_4$) C, H, N.

4-(8-Bromo-6-chloro-4-oxo-chroman-2-yl)butanoic Acid (10b). To a solution of **6b** (935 mg, 2.80 mmol) in dry CH_2Cl_2 (40 mL) Dess−Martin periodinane (1.82 g, 4.16 mmol) was added. The mixture was stirred for 45 min at room temperature. The reaction was quenched by the addition of 10% $Na_2S_2O_3$/$NaHCO_3$ (aq). After 5 min, the mix was diluted with CH_2Cl_2 and H_2O and the aqueous phase was extracted with CH_2Cl_2. The combined organic phases were washed with brine, dried over $MgSO_4$, filtered, and concentrated under reduced pressure. The crude aldehyde (1.14 g) was dissolved in THF (70 mL) and cooled to 0 °C. Amylene (1.96 g, 28.0 mmol) was added, and $NaClO_2$ (762 mg, 8.42 mmol) and $NaH_2PO_4{\cdot}2H_2O$ (875 mg, 5.61 mmol) dissolved in H_2O (33 mL) were added dropwise. The ice bath was removed, and the mixture was stirred for 2.5 h. The reaction was quenched by the addition of a mixture of 1 M HCl and brine (1:1) and EtOAc. After 5 min of stirring, the phases were separated and the aqueous phase was extracted with EtOAc. The combined organic phases were washed with brine/1 M HCl mix. The organic phase was extracted with 0.1 M NaOH. The basic aqueous phase was acidified with 1 M HCl (aq), and the acidic aqueous phase was extracted with EtOAc. The combined organic phases were finally washed with brine, dried over $MgSO_4$, filtered, and concentrated under reduced pressure. Flash chromatography was performed using EtOAc/heptane (3:7) with 1% AcOH to afford **10b** (716 mg, 74% over two steps) as an off-white solid; mp 123−124 °C. ^{1}H NMR (CD_3OD) δ 7.83 (d, J = 2.6 Hz, 1H), 7.75 (d, J = 2.5 Hz, 1H), 4.66−4.56 (m, 1H), 2.85−2.70 (m, 2H), 2.43 (t, J = 7.1 Hz, 2H), 2.05−1.76 (m, 4H). ^{13}C NMR (CD_3OD) δ. 192.1, 177.1, 158.2, 139.2, 127.7, 126.4, 123.8, 113.9, 80.3, 43.1, 35.0, 34.4, 21.8. Anal. ($C_{13}H_{12}BrClO_4$) C, H, N.

General Procedure for the Synthesis of Amides 11a−e. A 0.14 M solution of the appropriate carboxylic acid (1 equiv) in dry CH_2Cl_2 containing 5−10 vol % DMF was cooled to 0 °C under inert atmosphere. *N,N′*-Carbonyldiimidazole (1.5 equiv) was added, and the mixture was stirred for 30 min. The appropriate amine (3 equiv) was added, and the mixture was stirred at room temperature for 2−14 h. The mixture was diluted with CH_2Cl_2 and washed with 1 M HCl (aq) and brine, dried over $MgSO_4$, filtered, and concentrated under reduced pressure. Purification by flash chromatography gave the amides **11a−e**.

3-(8-Bromo-6-chloro-4-oxochroman-2-yl)-N-methylpropanamide (11a). The title compound was synthesized according to the general procedure from **10a** (99 mg, 0.30 mmol), methylamine hydrochloride (62 mg, 0.91 mmol), and *N,N′*-carbonyldiimidazole (73 mg, 1.52 mmol). Flash chromatography was performed using MeOH/CH_2Cl_2 (3:97) to afford **11a** (70 mg, 68%) as a white solid; mp 178−180 °C. ^{1}H NMR ($CDCl_3$) δ 7.81 (d, J = 2.4 Hz, 1H), 7.70 (d, J = 2.5 Hz, 1H), 5.63 (br s, 1H), 4.61−4.51 (m, 1H), 2.86−2.66 (m, 5H), 2.51 (app t, 2H), 2.26−2.07 (m, 2H). ^{13}C NMR ($CDCl_3$) δ 190.1, 172.2, 156.3, 138.5, 127.3, 126.1, 122.6, 112.6, 78.0, 42.5, 31.6, 30.4, 26.6. Anal. ($C_{13}H_{13}BrClNO_3$) C, H, N.

4-(8-Bromo-6-chloro-4-oxochroman-2-yl)-N-methylbutanamide (11b). The title compound was synthesized according to the general procedure from **10b** (100 mg, 0.28 mmol), methyl amine hydrochloride (60 mg, 0.89 mmol), and *N,N′*-carbonyldiimidazole (72 mg, 0.44 mmol). Flash chromatography was performed using MeOH/CH_2Cl_2 (3:97) to afford **2b** (96 mg, 93%) as a white solid; mp 136−139 °C. ^{1}H NMR ($CDCl_3$) δ 7.78 (d, J = 2.6 Hz, 1H), 7.69 (d, J = 2.6 Hz, 1H), 5.62 (s, 1H), 4.59−4.46 (m, 1H), 2.81 (d, J = 4.6 Hz, 3H), 2.76−2.66 (m, 2H), 2.36−2.24 (m, 2H), 2.03−1.75 (m, 4H). ^{13}C NMR ($CDCl_3$) δ 190.4, 173.0, 156.6, 138.5, 127.1, 125.9, 122.5, 112.7, 79.0, 42.5, 35.8, 34.1, 26.5, 21.4. Anal. Calcd for $C_{14}H_{15}BrClNO_3$ C, 46.63; H, 4.19; N, 3.88. Found: C, 47.28; H, 4.23; N, 3.78.

4-(8-Bromo-6-chloro-4-oxochroman-2-yl)-N-isopropylbutanamide (11c). The title compound was synthesized according to the general procedure from **10b** (100 mg, 0.28 mmol), *iso*-propylamine (76 μL, 0.89 mmol), and *N,N′*-carbonyldiimidazole (72 mg, 0.44 mmol). Flash chromatography was performed using MeOH/CH_2Cl_2 (3:97) to afford **11c** (97 mg, 84%) as an off-white solid; mp 151−154 °C. ^{1}H NMR ($CDCl_3$) δ 7.81 (d, J = 2.6 Hz, 1H), 7.70 (d, J = 2.5 Hz, 1H), 5.29 (s, 1H), 4.63−4.44 (m, 1H), 4.17−4.00 (m, 1H), 2.79−2.66 (m, 2H), 2.32−2.22 (m, 2H), 2.05−1.75 (m, 4H), 1.15 (d, J = 6.5 Hz, 6H). ^{13}C NMR ($CDCl_3$) δ 190.5, 171.4, 156.6, 138.5, 127.2, 126.0, 122.5, 112.8, 79.1, 42.5, 41.5, 36.1, 34.0, 23.02, 23.00, 21.5. Anal. ($C_{16}H_{19}BrClNO_3$) C, H, N.

N-Benzyl-4-(8-bromo-6-chloro-4-oxochroman-2-yl)butanamide (11d). The title compound was synthesized according to the general procedure from **10b** (85 mg, 0.24 mmol), benzyl amine (80 μL, 0.73 mmol), and *N,N′*-carbonyldiimidazole (60 mg, 0.37 mmol). Flash chromatography was performed using EtOAc/heptane (1:1 → 7:3 stepwise) and EtOAc/heptane (6:4 → 8:2) to afford **11d** (81 mg, 76%) as a pale-yellow solid; mp 128−131 °C. ^{1}H NMR ($CDCl_3$) δ 7.79 (d, J = 2.6 Hz, 1H), 7.69 (d, J = 2.6 Hz, 1H), 7.37−7.23 (m, 5H),

5.85 (s, 1H), 4.57−4.47 (m, 1H), 4.45 (d, J = 5.6 Hz, 2H), 2.76−2.64 (m, 2H), 2.42−2.30 (m, 2H), 2.10−1.75 (m, 4H). ^{13}C NMR ($CDCl_3$) δ 190.4, 172.2, 156.6, 138.5, 138.3, 128.9, 128.0, 127.7, 127.2, 126.0, 122.5, 112.8, 79.0, 43.8, 42.5, 35.9, 34.0, 21.5. HRMS $[M + H]^+$ calcd for $C_{20}H_{19}BrClNO_3$, 436.0315; found, 436.0315.

4-(8-Bromo-6-chloro-4-oxochroman-2-yl)-N,N-dimethylbutanamide (11e). The title compound was synthesized according to the general procedure from **10b** (100 mg, 0.28 mmol), dimethylamine hydrochloride (72 mg, 0.89 mmol), and *N,N′*-carbonyldiimidazole (71 mg, 0.44 mmol). Flash chromatography was performed using MeOH/CH_2Cl_2 (2:98) to afford **11e** (82 mg, 76%) as a colorless oil. ^{1}H NMR ($CDCl_3$) δ 7.77 (d, J = 2.6 Hz, 1H), 7.68 (d, J = 2.7 Hz, 1H), 4.59−4.47 (m, 1H), 3.01 (s, 3H), 2.94 (s, 3H), 2.78−2.65 (m, 2H), 2.50−2.35 (m, 2H), 2.04−1.78 (m, 4H). ^{13}C NMR ($CDCl_3$) δ 190.5, 172.3, 156.7, 138.4, 127.0, 125.9, 122.4, 112.8, 79.1, 42.4, 37.3, 35.5, 34.3, 32.7, 20.7. Anal. ($C_{15}H_{17}BrClNO_3$) C, H, N.

8-Bromo-6-chloro-2-(2-(3-methyl-1,2,4-oxadiazol-5-yl)-ethyl)chroman-4-one (12a). To a solution of **10a** (100 mg, 0.30 mmol) in MeCN (3 mL) and DMF (0.6 mL) were added *N,N′*-carbonyldiimidazole (73 mg, 0.45 mmol) and acetamide oxime (34 mg, 0.45 mmol). The mixture was heated to 85 °C for 19 h. EtOAc and water were added, and the aqueous phase was extracted with EtOAc. The combined organic phases were washed with 1% NaOH (aq) and brine, dried over $MgSO_4$, filtered, and concentrated under reduced pressure. Flash chromatography was performed using MeOH/CH_2Cl_2 (2:98) to afford **12a** (76 mg, 68%) as a yellow oil. ^{1}H NMR ($CDCl_3$) δ 7.79 (d, J = 2.6 Hz, 1H), 7.70 (d, J = 2.5 Hz, 1H), 4.71−4.57 (m, 1H), 3.31−3.11 (m, 2H), 2.82−2.71 (m, 2H), 2.48−2.35 (m, 1H), 2.37 (s, 3H), 2.34−2.23 (m, 1H). ^{13}C NMR ($CDCl_3$) δ 189.7, 178.3, 167.3, 156.2, 138.6, 127.5, 125.9, 122.4, 112.9, 77.4, 42.4, 31.3, 22.4, 11.7. Anal. ($C_{14}H_{12}BrClN_2O_3$) C, H, N.

8-Bromo-6-chloro-2-(3-(3-methyl-1,2,4-oxadiazol-5-yl)-propyl)chroman-4-one (12b). To a solution of **10b** (154 mg, 0.44 mmol) in MeCN (4.5 mL) and DMF (0.4 mL) were added *N,N′*-carbonyldiimidazole (108 mg, 0.66 mmol) and acetamide oxime (50 mg, 0.66 mmol). The mixture was heated to 85 °C for 14 h. EtOAc and water were added, and the aqueous phase was extracted with EtOAc. The combined organic phases were washed with 1% NaOH (aq) and brine, dried over $MgSO_4$, filtered, and concentrated under recued pressure. Flash chromatography was performed using MeOH/CH_2Cl_2 (3:97) to afford **12b** (86 mg, 50%) as a yellow oil. ^{1}H NMR ($CDCl_3$) δ 7.77 (d, J = 2.7 Hz, 1H), 7.68 (d, J = 2.6 Hz, 1H), 4.60−4.48 (m, 1H), 3.08−2.92 (m, 2H), 2.78−2.65 (m, 2H), 2.36 (s, 3H), 2.28−1.94 (m, 3H), 1.93−1.79 (m, 1H). ^{13}C NMR ($CDCl_3$) δ 190.1, 178.9, 167.2, 156.5, 138.5, 127.2, 125.9, 122.4, 112.8, 78.5, 42.4, 33.8, 26.1, 22.3, 11.7. Anal. ($C_{15}H_{14}BrClN_2O_3$) C, H, N.

3-Morpholinopropanal (13). Morpholine (1.63 mL, 18.67 mmol) and acrolein (1.50 mL, 22.42 mmol) were added to a suspension of $MgSO_4$ in MeCN (50 mL), and the reaction mixture was stirred overnight. $MgSO_4$ was filtered off, and the filtrate was concentrated under reduced pressure. The crude product was coevaporated with MeCN to afford **13** (2.45 g, 93%) as a yellow viscous oil which was used without further purification. ^{1}H NMR ($CDCl_3$) δ 9.77 (t, J = 2.0 Hz, 1H), 3.78−3.53 (m, 6H), 2.76−2.70 (m, 1H), 2.60−2.58 (m, 1H), 2.47−2.41 (m, 4H). ^{13}C NMR ($CDCl_3$) δ 201.6, 67.0, 53.6, 51.8, 41.1.

3-(*tert*-Butyldimethylsilyloxy)propanal (15). DMSO (0.60 mL, 8.46 mmol) was added dropwise to a solution of oxalyl chloride (0.37 mL, 4.24 mmol) in dry THF (30 mL) under N_2 atmosphere at −78 °C. The reaction mixture was stirred for 40 min, followed by the dropwise addition of 3-(*tert*-butyldimethylsilyl)oxy-1-propanol (700 mg, 3.68 mmol) in dry THF (12 mL). The mixture was stirred for additional 45 min at −78 °C. Et_3N (3 mL, 21.52 mmol) was added dropwise, and the mixture was stirred for 15 min at −78 °C and was then allowed to warm to room temperature. Water and CH_2Cl_2 were added, and the phases were separated. The aqueous phase was extracted with CH_2Cl_2, and the combined organic phases were washed with water and brine, dried over $MgSO_4$, filtered, and concentrated under reduced pressure. **15** (670 mg 97%) was afforded as a colorless oil which was used without further purification. ^{1}H NMR ($CDCl_3$) δ 9.80 (t, J = 2.1 Hz, 1H), 3.99 (t, J = 6.0 Hz, 2H), 2.59 (td, J = 6.0, 2.1 Hz, 2H), 0.88 (s, 9H), 0.06 (s, 6H). ^{13}C NMR ($CDCl_3$) δ 202.1, 57.6, 46.7, 26.0, 18.4, −5.3.

3-(8-Bromo-6-chloro-4-oxochroman-2-yl)propyl methanesulfonate (16). Mesyl chloride (52 μL, 0.67 mmol) was added to a solution of **6a** (150 mg, 0.47 mmol) and Et_3N (0.1 mL, 0.72 mmol) in dry CH_2Cl_2 (4 mL) at 0 °C under inert atmosphere. The mixture was stirred for 2 h and was then washed with water and brine, dried over $MgSO_4$, filtered, and concentrated under reduced pressure to afford **16** (180 mg, 96%) as a yellow solid. The product was used in the next step without further purification. ^{1}H NMR ($CDCl_3$) δ 7.82 (d, J = 2.5 Hz, 1H), 7.72 (d, J = 2.6 Hz, 1H), 4.60−4.50 (m, 1H), 4.46−4.31 (m, 2H), 3.04 (s, 3H), 2.80−2.69 (m, 2H), 2.26−1.84 (m, 4H). ^{13}C NMR ($CDCl_3$) δ 190.0, 156.4, 138.6, 127.4, 126.0, 122.5, 112.8, 78.4, 69.3, 42.6, 46.1, 37.7, 31.0, 25.4.

8-Bromo-6-chloro-2-(3-morpholinopropyl)chroman-4-one (17a). Morpholine (50 μL, 0.57 mmol) was added to a solution of **16** (96 mg, 0.24 mmol) in dry THF (2.5 mL). The mixture was heated by microwave irradiation to 100 °C for 40 min and 150 °C for 25 min. The mixture was concentrated under reduced pressure, and flash column chromatography was performed using MeOH/CH_2Cl_2 (5:95) followed by an acid−base extraction with 1 M HCl and NaOH (aq) to afford **17a** (48 mg, 51%) as a yellow oil. ^{1}H NMR ($CDCl_3$) δ 7.78 (d, J = 2.6 Hz, 1H), 7.68 (d, J = 2.6 Hz, 1H), 4.61−4.49 (m, 1H), 3.72−3.66 (m, 4H), 2.79−2.64 (m, 2H), 2.49−2.35 (m, 6H), 2.05−1.62 (m, 4H). ^{13}C NMR ($CDCl_3$) δ 190.5, 156.6, 138.5, 127.0, 125.9, 122.5, 112.8, 77.0, 67.1, 58.4, 53.8, 42.6, 32.6, 22.0. Anal. ($C_{16}H_{19}BrClNO_3$) C, H, N.

8-Bromo-6-chloro-2-(3-(piperidin-1-yl)propyl)chroman-4-one (17b). Piperidine (60 μL, 0.61 mmol) was added to a solution of **16** (101 mg, 0.25 mmol) in dry THF (2.5 mL). The mixture was heated by microwave irradiation at 120 °C for 1 h and concentrated under reduced pressure. Flash column chromatography was performed using MeOH/CH_2Cl_2 (5:95), followed by an acid−base extraction with 1 M HCl and NaOH (aq) to afford **17b** (38 mg, 39%) as a yellow oil. ^{1}H NMR ($CDCl_3$) δ 7.77 (d, J = 2.6 Hz, 1H), 7.68 (d, J = 2.6 Hz, 1H), 4.59−4.48 (m, 1H), 2.80−2.63 (m, 2H), 2.48−2.30 (m, 6H), 2.02−1.32 (m, 10H). ^{13}C NMR ($CDCl_3$) δ 190.6, 156.7, 138.5, 127.0, 125.9, 122.5, 112.8, 79.0, 58.8, 54.6, 42.5, 32.9, 25.9, 24.5, 22.3. Anal. ($C_{17}H_{21}BrClNO_2$) C, H, N.

3-(2-Oxo-1,2-dihydroquinolin-6-yl)propanal (19a). 6-Bromoquinolin-2(1*H*)-one (303.2 mg, 1.35 mmol), $Pd(OAc)_2$ (31 mg, 0.14 mmol), KCl (102 mg, 1.36 mmol), K_2CO_3 (282 mg, 2.04 mmol), and TBAA (820 mg, 2.71 mmol) were dissolved in dry DMF (6 mL) under inert atmosphere. Acrolein diethyl acetal (0.62 mL, 4.06 mmol) was added, and the mixture was heated at 90 °C overnight. The reaction was divided in three runs. The mixtures were diluted with EtOAc, filtered through Celite, rinsed with EtOAc, and concentrated under reduced pressure and coevaporated with toluene to afford **18a** as brown oil (1157 mg), which was used in the next step without further purification. **18a** was dissolved in MeOH (14 mL), and 10% Pd/C (10 wt %, 111 mg) was added. The mixture was stirred under H_2 atmosphere (balloon) for 3 h at room temperature, filtered through Celite, and the filtrate was concentrated under reduced pressure, resulting in a brown oil (960 mg). The crude oil was dissolved acetone (13 mL), whereafter water (0.6 mL) and HCl (0.5 mL, conc) were added. The mixture was heated to reflux for 4 h. The solvent was removed, and EtOAc and water were added to the residue. The phases were separated, and the aqueous phase was extracted with EtOAc. The combined organic phases were washed with saturated $NaHCO_3$ (aq), water and brine, dried over Na_2SO_4, filtered, and concentrated under reduced pressure. The crude product was purified by flash column chromatography using MeOH/EtOAc (3:97) as eluent, affording the **19a** as a pale-yellow solid (97 mg, 34% over three steps); mp 139−141 °C. ^{1}H NMR (acetone-d_6) δ 11.47 (br s, 1H), 9.80 (t, J = 1.3 Hz, 1H), 7.85 (d, J = 9.5 Hz, 1H), 7.52 (d, J = 2.1 Hz, 1H), 7.44 (dd, J = 8.4, 2.0 Hz, 1H), 7.34 (d, J = 8.4 Hz, 1H), 6.55 (d, J = 9.5 Hz, 1H), 2.99 (app t, 2H), 2.86−2.79 (m, 2H). ^{13}C NMR (acetone-d_6) δ 202.0, 163.5, 141.1, 138.4, 135.8, 131.9, 128.0, 122.8, 120.5, 116.3, 45.8, 28.0.

dx.doi.org/10.1021/jm500930h | J. Med. Chem. 2014, 57, 9870−9888

3-(Quinolin-6-yl)propanal (19b). 6-Bromoquinoline (106 mg, 0.51 mmol) was dissolved in dry DMF (2 mL) under inert atmosphere, and $Pd(OAc)_2$ (12 mg, 0.054 mmol), KCl (38 mg, 0.51 mmol), K_2CO_3 (108 mg, 0.78 mmol), and TBAA (311 mg, 1.02 mmol) were added. Acrolein diethyl acetal (0.23 mL, 1.53 mmol) was added, and the mixture was heated at 90 °C for 24 h. The reaction was divided in three runs in the microwave. The mixtures were diluted with EtOAc, filtered through Celite, rinsed with EtOAc, and concentrated under reduced pressure and coevaporated with toluene to afford **18b** as brown oil (471 mg), which was used in the next step without further purification. **18b** was dissolved EtOH (10 mL), and 1,4-cyclohexadiene (0.48 mL, 10 mmol) and 10% Pd/C (11 mg, 0.01 mmol) were added. The mixture was heated to reflux for 1.5 h. Two subsequent additions of 1,4-cyclohexadiene (0.23 mL, 2.5 mmol; 0.48 mL, 5.1 mmol) and 10% Pd/C (11 mg, 0.01 mmol and 8 mg, 0.007 mmol) were made after 1.5 and 3 h of heating. The mixture was heated to reflux for 4.5 h in total. The mixture was diluted with EtOAc, filtered through Celite, rinsed with EtOAc, and concentrated under reduced pressure, affording the crude product as a yellow oil (374 mg). The crude oil was dissolved acetone (13 mL), whereafter water (2 mL) and HCl (1 mL, conc) were added. The mixture was heated to reflux for 2 h. The solvent was removed, and EtOAc and saturated Na_2CO_3 (aq) were added to the residue. The phases were separated, and the aqueous phase was extracted with EtOAc. The combined organic phases were washed with saturated $NaHCO_3$ (aq), water, and brine, dried over $MgSO_4$, filtered, and concentrated under reduced pressure. The crude product was purified by flash column chromatography using EtOAc as eluent to afford **19b** as a transparent oil (53 mg, 56% over three steps). ^{1}H NMR ($CDCl_3$) δ 9.82 (t, J = 1.3 Hz, 1H), 8.84 (dd, J = 4.2, 1.8 Hz, 1H), 8.05 (ddd, J = 8.4, 1.9, 0.8 Hz, 1H), 8.01 (d, J = 8.6 Hz, 1H), 7.57 (d, J = 1.4 Hz, 1H), 7.53 (dd, J = 8.6, 2.0 Hz, 1H), 7.34 (dd, J = 8.3, 4.2 Hz, 1H), 3.11 (t, J = 7.5 Hz, 2H), 2.85 (tdd, J = 7.6, 1.3, 0.5 Hz, 2H). ^{13}C NMR ($CDCl_3$) δ 201.1, 150.1, 147.3, 138.8, 135.6, 130.6, 129.8, 128.4, 126.4, 121.3, 45.0, 28.0.

6-(2-(8-Bromo-6-chloro-4-oxochroman-2-yl)ethyl)quinolin-2(1*H*)-one (20a). 3′-Bromo-5′-chloro-2′-hydroxyacetophenone (58 mg, 0.23 mmol) was dissolved in EtOH (1 mL), DIPA (32 μmL, 0.23 mmol) and **19a** (42 mg, 0.21 mmol) were added to a microwave vial, and the mixture was heated in the microwave to 160 °C for 1.5 h. The formed brown precipitate was filtered off, rinsed with EtOAc, and triturated with CH_2Cl_2, resulting in a pale-yellow solid (44 mg, 49%); mp 229–231 °C. ^{1}H NMR (DMSO-d_6) δ 11.67 (br s, 1H), 8.04 (d, J = 2.6 Hz, 1H), 7.83 (d, J = 9.5 Hz, 1H), 7.67 (d, J = 2.6 Hz, 1H), 7.53 (d, J = 2.0 Hz, 1H), 7.41 (dd, J = 8.4, 2.0 Hz, 1H), 7.23 (d, J = 8.4 Hz, 1H), 6.46 (d, J = 9.5 Hz, 1H), 4.69–4.56 (m, 1H), 3.03–2.72 (m, 4H), 2.25–1.94 (m, 2H). ^{13}C NMR (DMSO-d_6) δ 190.2, 161.8, 156.2, 140.0, 137.7, 137.3, 134.2, 130.9, 127.0, 125.6, 125.0, 122.5, 121.9, 119.1, 115.2, 112.6, 77.8, 41.4, 35.4, 29.8. HRMS (ESI-LC/MS) $[M + H]^+$: calcd for $C_{20}H_{15}BrClNO_3$, 432.0002; found, 432.0025.

8-Bromo-6-chloro-2-(2-(quinolin-6-yl)ethyl)chroman-4-one (20b). 3′-Bromo-5′-chloro-2′-hydroxyacetophenone (77.1 mg, 0.31 mmol) was dissolved in EtOH (1 mL), DIPA (44 μL, 0.31 mmol) and **19b** (52 mg, 0.28 mmol) were added to a microwave vial, and the mixture was heated in the microwave reactor to 170 °C for 2 h. The solvent was removed, and the residue was redissolved in EtOAc. The organic phase was washed with 10% NaOH (aq), water, and brine, dried over $MgSO_4$, filtered, and concentrated under reduced pressure. The crude product was purified by flash column chromatography using EtOAc/pentane (1:1) as eluent, affording **20b** as a pale-yellow solid (18 mg, 15%); mp 187–190 °C. ^{1}H NMR ($CDCl_3$) δ 8.88 (d, J = 4.2 Hz, 1H), 8.10 (dd, J = 8.3, 1.2 Hz, 1H), 8.06 (d, J = 8.7 Hz, 1H), 7.80 (d, J = 2.6 Hz, 1H), 7.74 (d, J = 2.6 Hz, 1H), 7.69 (d, J = 1.9 Hz, 1H), 7.63 (dd, J = 8.6, 2.0 Hz, 1H), 7.39 (dd, J = 8.3, 4.2 Hz, 1H), 4.55–4.41 (m, 1H), 3.30–3.01 (m, 2H), 2.84–2.68 (m, 2H), 2.45–2.32 (m, 1H), 2.19–2.03 (m, 1H). ^{13}C NMR ($CDCl_3$) δ 190.2, 156.5, 150.2, 147.4, 139.0, 138.6, 135.7, 130.8, 129.9, 128.4 [determined by ^{1}H–^{13}C heteronuclear multiple-bond (HMBC) spectroscopy], 127.3, 126.8, 126.0, 122.6, 121.5, 112.9, 77.6, 42.6, 36.2, 31.2. Anal. ($C_{20}H_{15}BrClNO_2 \cdot 0.3H_2O$) C, H, N.

***N*-(8-Bromo-6-chloro-4-oxo-2-phenethyl-4*H*-chromen-3-yl)-acetamide (23).** Compound **22** was dissolved in pyridine (2 mL), and acetic anhydride (55 μL, 0.6 mmol) was added. The mixture was stirred at room temperature overnight. The solution was coevaporated with toluene and EtOH. Purification by flash chromatography EtOAc:heptane (4:6) gave **23** (0.19 g, 87%) as a white solid; mp 203 °C. ^{1}H NMR ($CDCl_3$) δ 8.09 (d, J = 2.6 Hz, 1H), 7.89 (d, J = 2.6 Hz, 1H), 7.32–7.17 (m, 5H), 6.91 (bs, 1H), 3.22–3.05 (m, 4H), 2.19 (s, 3H). ^{13}C NMR δ 189.2, 173.1, 169.3, 165.1, 151.0, 140.2, 136.9, 131.2, 128.7, 128.5, 126.6, 124.7, 124.3, 119.8, 112.8, 100.0, 34.1, 32.1, 23.6. Anal. ($C_{19}H_{15}BrClNO_3$) C, H, N.

(*Z*)-3-(Aminomethylene)-8-bromo-6-chloro-2-phenethylchroman-4-one (25). A solution of **24** (0.025 g, 0.06 mmol) in anhydrous THF (2 mL) was cooled to −78 °C, and DIBAL-H (0.06 mL, 0.06 mmol, 1 M in CH_2Cl_2) was added dropwise to the mixture. After 1 h at −78 °C, a further portion of DIBAL-H (0.06 mL, 0.06 mmol, 1 M in CH_2Cl_2) was added. After 2 h, the reaction was quenched with saturated NH_4Cl (aq), followed by the addition of EtOAc. The aqueous phase was extracted three times with EtOAc, and the combined organic phases were washed with H_2O and brine. The organic phase was dried over $MgSO_4$ and concentrated under vacuum. Purification by flash chromatography using EtOAc:heptane (2:8 → 4:6) gave **25** (17 mg, 66%) as a beige solid; mp 106–108 °C. ^{1}H NMR ($CDCl_3$) δ 9.24 (br d, J = 10.3 Hz, 1H), 7.80 (d, J = 2.6 Hz, 1H), 7.61 (d, J = 2.6 Hz, 1H), 7.34–7.15 (m, 5H), 6.86–6.78 (m, 1H), 5.22 (br s, 1H), 4.86 (dd, J = 9.9, 4.4 Hz, 1H) 2.88–2.71 (m, 2H), 2.28–2.15 (m, 1H), 1.86–1.73 (m, 1H). ^{13}C NMR ($CDCl_3$) δ 180.9, 153.3, 147.5, 141.0, 136.6, 128.74, 128.66, 126.9, 126.2, 125.7, 125.3, 112.5, 102.8, 79.2, 37.6, 31.8. The compound is 97% pure according to HPLC analysis.

In Vitro Fluor de Lys Assay for SIRT1–3 Activities. The Fluor de Lys fluorescence assays were based on the method described in the BioMol product sheet (Enzo Life Sciences) using the BioMol KI177 substrate for SIRT1 and the KI179 substrate for SIRT2 and SIRT3. The determined K_m value of SIRT1 for KI177 was 58 μM, and the K_m of SIRT2 for KI179 was 198 μM.[77] The K_m of SIRT3 for KI179 was reported by BioMol to be 32 μM. The K_m values of SIRT1, SIRT2, and SIRT3 for NAD^+ were reported by BioMol to be 558 μM, 547 μM, and 2 mM, respectively.

Briefly, assays were carried out using the Fluor de Lys acetylated peptide substrate at a concentration corresponding to 0.7 K_m and NAD^+ (N6522, Sigma) at a concentration corresponding to 0.9 K_m, recombinant GST-SIRT1/2-enzyme or recombinant His-SIRT3 and SIRT assay buffer (HDAC assay buffer, KI143, supplemented with 1 mg/mL BSA, A3803, Sigma). GST-SIRT1 and GST-SIRT2 were produced as described previously.[78,79] His-SIRT3 (BML-SE270) was purchased from Enzo Life Sciences. The buffer, Fluor de Lys acetylated peptide substrate, NAD^+, and DMSO/compounds in DMSO (2.5 μL in 50 μL total reaction volume; DMSO from Sigma, D2650) were preincubated for 5 min at room temperature. The reaction was started by adding the enzyme. The reaction mixture was incubated for 1 h at 37 °C. After that, Fluor de Lys developer (KI176) and nicotinamide (2 mM in HDAC assay buffer giving total volume of 50 μL) were added, and the incubation was continued for 45 min at 37 °C. Fluorescence readings were obtained using EnVision 2104 multilabel reader (PerkinElmer) with excitation wavelength 370 nm and emission 460 nm.

The IC_{50} values were determined as three independent determinations with 8–10 different inhibitor concentrations in each determination. This gave altogether 27 data points that were included in the calculation of the best-fit value for nonlinear curve fitting with GraphPad Prism5 (GraphPad Software, Inc.).

Histone Deacetylase (HDAC) Activity Assay. The assay was done according to the instructions of the HDAC fluorimetric assay/drug discovery kit (AK500, Enzo). Briefly, the assay was carried out using 50 μM Fluor de Lys HDAC substrate (KI104, Enzo) and 200 μM test compounds with HeLa cell nuclear extract (KI410, Enzo) as a source of HDAC enzymatic activity. The reaction mixture was incubated for 1 h at 37 °C. After that, Fluor de Lys developer plus 1 μM Trichostatin A was added and incubation was continued for 15

min at 25 °C. Fluorescence readings were obtained with EnVision 2104 multilabel reader (PerkinElmer) with excitation wavelength 370 nm and emission 460 nm.

SIRTainty Sirtuin Activity Assay. The fluorometric SIRTainty class III HDAC assay (Millipore) employs nicotinamidase to measure nicotinamide generated upon the cleavage of NAD^+ during sirtuin mediated deacetylation of a substrate.[80] The SIRT2 activity testing was performed according to the assay instructions in the presence and absence of NAD^+. The results were read using Victor 1420 multilabel counter (Wallac) with excitation wavelength 405 nm and emission 460 nm and were reported as % of inhibition of the NAD^+-dependent signal.

Cell Culture. Human A549 lung carcinoma cells and MCF-7 breast carcinoma cells (both from ATCC) were maintained in Dulbecco's Modified Eagle Medium (DMEM) containing 10% fetal calf serum, 100 U/mL penicillin, and 100 μg/mL streptomycin (all from Gibco) at +37 °C in a humidified atmosphere of 5% CO_2/95% air.

Cell Proliferation and Cell Cycle Analysis. For cell proliferation assays with sulforhodamine B, the cells were plated to 96-well plates (Nunc) 24 h before the start of the treatments (3000 cells/well). The cells were treated with vehicle (0.5% DMSO) or test compounds for 48 h (A549 cells) or 72 h (MCF-7 cells). Sulforhodamine B staining was performed as previously described.[64] For cell cycle analysis with propidium iodide staining, the cells were plated to 6-well plates (Nunc) 6 h before the start of the treatments (0.6×10^6 cells/well). The cells were treated with vehicle (0.5% DMSO) or test compounds for 18 h. Propidium iodide staining was performed as previously described.[64] FACScanto II flow cytometer with FACSDiva software (Becton Dickinson) was used to analyze cellular DNA content and cell cycle.

Western Blotting. The MCF-7 cells were plated to 12-well plates (Nunc) at a density of 10^5 cells/well, and the experiments were initiated after 24 h. The cells were treated with vehicle (0.5% DMSO) or test compounds as previously described.[81] For the analysis of α-tubulin acetylation levels, the cells were lysed into M-PER mammalian protein extraction reagent (Thermo Fisher Scientific) followed by centrifugation (20 min, 16000*g*, +4 °C). After electrophoretic separation in SDS-PAGE gel, the proteins were transferred onto Hybond-ECL nitrocellulose transfer membrane (GE Healthcare) and were detected with mouse monoclonal acetylated α-tubulin antibody (T6793, Sigma) and total α-tubulin antibody (T5168, Sigma). The protein signals were visualized with peroxidase-conjugated sheep antimouse secondary antibody (ab97046, Abcam) and ECL Plus chemiluminescent substrate (GE Healthcare). The images were obtained by the use of digital imaging (ImageQuant, GE Healthcare).

Statistical Analyses. Statistical differences between groups were tested using one-way analysis of variance (ANOVA), followed by Tukey's Multiple Comparison Test, with $p < 0.05$ considered as statistically significant. Data analysis was performed using GraphPad Prism version 5.03 for Windows (GraphPad Software).

■ ASSOCIATED CONTENT

Supporting Information

Characterization data and elemental analysis or HRMS analyses for all tested compounds; complete list of SIRT1−3 activity assay results; list of calculated physicochemical properties of all tested compounds; description of the SIRT2 homology modeling procedure and validation; ^1H NMR and ^{13}C NMR spectra of all compounds. This material is available free of charge via the Internet at http://pubs.acs.org.

■ AUTHOR INFORMATION

Corresponding Authors

*For K.L.: phone, +46 31 786 9031; fax, +46 31 772 1394; E-mail, luthman@chem.gu.se.

*For E.M.J.: phone, +358 40 355 2460; fax, +358 17 162424; E-mail, Elina.Jarho@uef.fi.

Notes

The authors declare no competing financial interest.

■ ACKNOWLEDGMENTS

We thank the Swedish Research Council (project no. 621-2013-4749), the Academy of Finland (grant nos. 127062 and 132780), and the Department of Chemistry and Molecular Biology, University of Gothenburg, for financial support and Biocenter Kuopio for providing facilities. We also thank Johanna Stéen for skillful assistance in the lab. This work is part of COST Action TD09056: "Epigenetics: Bench to Bedside".

■ ABBREVIATION USED

Ac, acetyl; ADP, adenosine diphosphate; ADPr, adenosine diphosphate ribose; ANOVA, analysis of variance; BSA, bovine serum albumin; DDQ, 2,3-dichloro-5,6-dicyano-*p*-benzoquinone; DIBAL-H, diisobutylaluminum hydride; DIPA, *N*,*N*-diisopropylamine; DMF, dimethylformamide; DMSO, dimethyl sulfoxide; DNA, deoxyribnucleic acid; ECL, enhanced chemiluminescence; ESI-MS, electrospray ionization mass spectrometry; FOX, Forkhead box protein; GST, glutathione-*S*-transferase; HDAC, histone deacetylase; HPLC, high-performance liquid chromatography; IC_{50}, the half-maximal inhibitory concentration; KHMDS, potassium bis(trimethylsilyl)amide; LDA, lithium diisopropylamide; LDS, lithium dodecyl sulfate; Ms, methanesulfonyl; MW, microwave; NAD^+, nicotinamide adenine dinucleotide; NMR, nuclear magnetic resonance; PDB, Protein Data Bank; SAR, structure−activity relationship; SDS-PAGE, sodium dodecyl sulfate polyacrylamide gel electrophoresis; SEM, standard error of the mean; SIRT, silent information regulator type; TBAA, tetra-*N*-butylammonium acetate; TBDMS, *tert*-butyldimethylsilyl; TEMPO, (2,2,6,6-tetramethylpiperidin-1-yl)oxy; THF, tetrahydrofuran; TLC, thin-layer chromatography; TPAP, tetrapropylammonium perruthenate; Ts, tosyl; *p*-TSA, *p*-toluenesulfonic acid; UV, ultraviolet

■ REFERENCES

(1) Michishita, E.; Park, J. Y.; Burneskis, J. M.; Barrett, J. C.; Horikawa, I. Evolutionarily conserved and nonconserved cellular localizations and functions of human SIRT proteins. *Mol. Biol. Cell* **2005**, *16*, 4623−4635.

(2) Nakagawa, T.; Guarente, L. Sirtuins at a glance. *J. Cell Sci.* **2011**, *124*, 833−838.

(3) Imai, S.; Armstrong, C. M.; Kaeberlein, M.; Guarente, L. Transcriptional silencing and longevity protein Sir2 is an NAD-dependent histone deacetylase. *Nature* **2000**, *403*, 795−800.

(4) Sauve, A. A.; Celic, I.; Avalos, J.; Deng, H. T.; Boeke, J. D.; Schramm, V. L. Chemistry of gene silencing: the mechanism of NAD(+)-dependent deacetylation reactions. *Biochemistry* **2001**, *40*, 15456−15463.

(5) Jackson, M. D.; Schmidt, M. T.; Oppenheimer, N. J.; Denu, J. M. Mechanism of nicotinamide inhibition and transglycosidation by Sir2 histone/protein deacetylases. *J. Biol. Chem.* **2003**, *278*, 50985−50998.

(6) Liszt, G.; Ford, E.; Kurtev, M.; Guarente, L. Mouse Sir2 homolog SIRT6 is a nuclear ADP-ribosyltransferase. *J. Biol. Chem.* **2005**, *280*, 21313−21320.

(7) Jiang, H.; Khan, S.; Wang, Y.; Charron, G.; He, B.; Sebastian, C.; Du, J. T.; Kim, R.; Ge, E.; Mostoslavsky, R.; Hang, H. C.; Hao, Q.; Lin, H. N. SIRT6 regulates TNF-alpha secretion through hydrolysis of long-chain fatty acyl lysine. *Nature* **2013**, *496*, 110−113.

(8) Feldman, J. L.; Baeza, J.; Denu, J. M. Activation of the protein deacetylase SIRT6 by long-chain fatty acids and widespread

deacylation by mammalian sirtuins. *J. Biol. Chem.* **2013**, *288*, 31350−31356.
(9) Ahuja, N.; Schwer, B.; Carobbio, S.; Waltregny, D.; North, B. J.; Castronovo, V.; Maechler, P.; Verdin, E. Regulation of insulin secretion by SIRT4, a mitochondrial ADP-ribosyltransferase. *J. Biol. Chem.* **2007**, *282*, 33583−33592.
(10) Du, J. T.; Zhou, Y. Y.; Su, X. Y.; Yu, J. J.; Khan, S.; Jiang, H.; Kim, J.; Woo, J.; Kim, J. H.; Choi, B. H.; He, B.; Chen, W.; Zhang, S.; Cerione, R. A.; Auwerx, J.; Hao, Q.; Lin, H. N. Sirt5 is a NAD-dependent protein lysine demalonylase and desuccinylase. *Science* **2011**, *334*, 806−809.
(11) Tan, M. J.; Peng, C.; Anderson, K. A.; Chhoy, P.; Xie, Z. Y.; Dai, L. Z.; Park, J.; Chen, Y.; Huang, H.; Zhang, Y.; Ro, J.; Wagner, G. R.; Green, M. F.; Madsen, A. S.; Schmiesing, J.; Peterson, B. S.; Xu, G. F.; Ilkayeva, O. R.; Muehlbauer, M. J.; Braulke, T.; Muhlhausen, C.; Backos, D. S.; Olsen, C. A.; McGuire, P. J.; Pletcher, S. D.; Lombard, D. B.; Hirschey, M. D.; Zhao, Y. M. Lysine glutarylation is a protein posttranslational modification regulated by SIRT5. *Cell Metab.* **2014**, *19*, 605−617.
(12) Michan, S.; Sinclair, D. Sirtuins in mammals: insights into their biological function. *Biochem. J.* **2007**, *404*, 1−13.
(13) Herskovits, A. Z.; Guarente, L. Sirtuin deacetylases in neurodegenerative diseases of aging. *Cell Res.* **2013**, *23*, 746−758.
(14) Morris, B. J. Seven sirtuins for seven deadly diseases of aging. *Free Radical Biol. Med.* **2013**, *56*, 133−171.
(15) Smith, M. R.; Syed, A.; Lukacsovich, T.; Purcell, J.; Barbaro, B. A.; Worthge, S. A.; Wei, S. R.; Pollio, G.; Magnoni, L.; Scali, C.; Massai, L.; Franceschini, D.; Camarri, M.; Gianfriddo, M.; Diodato, E.; Thomas, R.; Gokce, O.; Tabrizi, S. J.; Caricasole, A.; Landwehrmeyer, B.; Menalled, L.; Murphy, C.; Ramboz, S.; Luthi-Carter, R.; Westerberg, G.; Marsh, J. L. A potent and selective Sirtuin 1 inhibitor alleviates pathology in multiple animal and cell models of Huntington's disease. *Hum. Mol. Genet.* **2014**, *23*, 2995−3007.
(16) A Phase II Safety and Tolerability Study With SEN0014196. *ClinicalTrials.gov*; U.S. National Library of Medicine, U.S. National Institutes of Health: Bethesda, MD, 2012; NCT01521585, https://clinicaltrials.gov/ct2/show/NCT01521585?term=nct01521585&rank=1.
(17) Dryden, S. C.; Nahhas, F. A.; Nowak, J. E.; Goustin, A. S.; Tainsky, M. A. Role for human SIRT2 NAD-dependent deacetylase activity in control of mitotic exit in the cell cycle. *Mol. Cell. Biol.* **2003**, *23*, 3173−3185.
(18) de Oliveira, R. M.; Sarkander, J.; Kazantsev, A. G.; Outeiro, T. F. SIRT2 as a therapeutic target for age-related disorders. *Front. Pharmacol.* **2012**, *3*, 82.
(19) Inoue, T.; Hiratsuka, M.; Osaki, M.; Oshimura, M. The molecular biology of mammalian SIRT proteins—SIRT2 in cell cycle regulation. *Cell Cycle* **2007**, *6*, 1011−1018.
(20) Taylor, D. M.; Balabadra, U.; Xiang, Z. M.; Woodman, B.; Meade, S.; Amore, A.; Maxwell, M. M.; Reeves, S.; Bates, G. P.; Luthi-Carter, R.; Lowden, P. A. S.; Kazantsev, A. G. A brain-permeable small molecule reduces neuronal cholesterol by inhibiting activity of sirtuin 2 deacetylase. *ACS Chem. Biol.* **2011**, *6*, 540−546.
(21) Chopra, V.; Quinti, L.; Kim, J.; Vollor, L.; Narayanan, K. L.; Edgerly, C.; Cipicchio, P. M.; Lauver, M. A.; Choi, S. H.; Silverman, R. B.; Ferrante, R. J.; Hersch, S.; Kazantsev, A. G. The sirtuin 2 inhibitor AK-7 is neuroprotective in Huntington's disease mouse models. *Cell Rep.* **2012**, *2*, 1492−1497.
(22) Outeiro, T. F.; Kontopoulos, E.; Altmann, S. M.; Kufareva, I.; Strathearn, K. E.; Amore, A. M.; Volk, C. B.; Maxwell, M. M.; Rochet, J. C.; McLean, P. J.; Young, A. B.; Abagyan, R.; Feany, M. B.; Hyman, B. T.; Kazantsev, A. G. Sirtuin 2 inhibitors rescue alpha-synuclein-mediated toxicity in models of Parkinson's disease. *Science* **2007**, *317*, 516−519.
(23) Park, S.-H.; Zhu, Y.; Ozden, O.; Kim, H.-S.; Jiang, H.; Deng, C.-X.; Gius, D.; Vassilopoulos, A. SIRT2 is a tumor suppressor that connects aging, acetylome, cell cycle signaling, and carcinogenesis. *Transl. Cancer Res.* **2012**, *1*, 15−21.
(24) Bosch-Presegué, L.; Vaquero, A. The dual role of sirtuins in cancer. *Genes Cancer* **2011**, *2*, 648−662.
(25) Roth, M.; Chen, W. Y. Sorting out functions of sirtuins in cancer. *Oncogene* **2014**, *33*, 1609−1620.
(26) He, X.; Nie, H.; Hong, Y. Y.; Sheng, C. B.; Xia, W. L.; Ying, W. H. SIRT2 activity is required for the survival of C6 glioma cells. *Biochem. Biophys. Res. Commun.* **2012**, *417*, 468−472.
(27) Li, Y. Z.; Matsumori, H.; Nakayama, Y.; Osaki, M.; Kojima, H.; Kurimasa, A.; Ito, H.; Mori, S.; Katoh, M.; Oshimura, M.; Inoue, T. SIRT2 down-regulation in HeLa can induce p53 accumulation via p38 MAPK activation-dependent p300 decrease, eventually leading to apoptosis. *Genes Cells* **2011**, *16*, 34−45.
(28) Xie, H. J.; Jung, K. H.; Nam, S. W. Overexpression of SIRT2 contributes tumor cell growth in hepatocellular carcinomas. *Mol. Cell. Toxicol.* **2011**, *7*, 367−374.
(29) Liu, P. Y.; Xu, N.; Malyukova, A.; Scarlett, C. J.; Sun, Y. T.; Zhang, X. D.; Ling, D.; Su, S. P.; Nelson, C.; Chang, D. K.; Koach, J.; Tee, A. E.; Haber, M.; Norris, M. D.; Toon, C.; Rooman, I.; Xue, C.; Cheung, B. B.; Kumar, S.; Marshall, G. M.; Biankin, A. V.; Liu, T. The histone deacetylase SIRT2 stabilizes Myc oncoproteins. *Cell Death Differ.* **2013**, *20*, 503−514.
(30) Di Fruscia, P.; Ho, K. K.; Laohasinnarong, S.; Khongkow, M.; Kroll, S. H. B.; Islam, S. A.; Sternberg, M. J. E.; Schmidtkunz, K.; Jung, M.; Lam, E. W. F.; Fuchter, M. J. The discovery of novel 10,11-dihydro-5*H*-dibenz[*b*,*f*]azepine SIRT2 inhibitors. *MedChemComm* **2012**, *3*, 373−378.
(31) Hoffmann, G.; Breitenbuecher, F.; Schuler, M.; Ehrenhofer-Murray, A. E. A novel Sirtuin 2 (SIRT2) inhibitor with p53-dependent pro-apoptotic activity in non-small-cell lung cancer. *J. Biol. Chem.* **2014**, *289*, 5208−5216.
(32) Fridén-Saxin, M.; Seifert, T.; Landergren, M. R.; Suuronen, T.; Lahtela-Kakkonen, M.; Jarho, E. M.; Luthman, K. Synthesis and evaluation of substituted chroman-4-one and chromone derivatives as sirtuin 2-selective inhibitors. *J. Med. Chem.* **2012**, *55*, 7104−7113.
(33) McDougal, P. G.; Rico, J. G.; Oh, Y. I.; Condon, B. D. A Convenient procedure for the monosilylation of symmetrical 1,*n*-diols. *J. Org. Chem.* **1986**, *51*, 3388−3390.
(34) Shah, S. T. A.; Singh, S.; Guiry, P. J. A Novel, Chemoselective and efficient microwave-assisted deprotection of silyl ethers with Selectfluor. *J. Org. Chem.* **2009**, *74*, 2179−2182.
(35) Heravi, M. M.; Ajami, D.; Tabar-Heydar, K. Oxidation of alcohols by montmorillonite K-10 supported bis(trimethylsilyl)-chromate. *Monatsh. Chem.* **1998**, *129*, 1305−1308.
(36) Tietze, L. F.; Schneider, C.; Pretor, M. Improved synthesis of (*E*)-3-alkoxy- and (*E*)-3-phenoxyacryloyl chlorides. *Synthesis* **1993**, 1079−1080.
(37) Zaragoza, F.; Stephensen, H.; Peschke, B.; Rimvall, K. 2-(4-Alkylpiperazin-1-yl)quinolines as a new class of imidazole-free histamine H-3 receptor antagonists. *J. Med. Chem.* **2005**, *48*, 306−311.
(38) Battistuzzi, G.; Cacchi, S.; Fabrizi, G. An efficient palladium-catalyzed synthesis of cinnamaldehydes from acrolein diethyl acetal and aryl iodides and bromides. *Org. Lett.* **2003**, *5*, 777−780.
(39) Quinn, J. F.; Razzano, D. A.; Golden, K. C.; Gregg, B. T. 1,4-Cyclohexadiene with Pd/C as a rapid, safe transfer hydrogenation system with microwave heating. *Tetrahedron Lett.* **2008**, *49*, 6137−6140.
(40) Fridén-Saxin, M.; Pemberton, N.; Andersson, K. D.; Dyrager, C.; Friberg, A.; Grøtli, M.; Luthman, K. Synthesis of 2-alkyl-substituted chromone derivatives using microwave irradiation. *J. Org. Chem.* **2009**, *74*, 2755−2759.
(41) Ankner, T.; Friden-Saxin, M.; Pemberton, N.; Seifert, T.; Grøtli, M.; Luthman, K.; Hilmersson, G. KHMDS enhanced SmI_2-mediated Reformatsky type α-cyanation. *Org. Lett.* **2010**, *12*, 2210−2213.
(42) Min, J. R.; Landry, J.; Sternglanz, R.; Xu, R. M. Crystal structure of a SIR2 homolog−NAD complex. *Cell* **2001**, *105*, 269−279.
(43) Sanders, B. D.; Jackson, B.; Marmorstein, R. Structural basis for sirtuin function: what we know and what we don't. *Biochim. Biophys. Acta, Proteins Proteomics* **2010**, *1804*, 1604−1616.

(44) Borra, M. T.; Langer, M. R.; Slama, J. T.; Denu, J. M. Substrate specificity and kinetic mechanism of the Sir2 family of NAD(+)-dependent histone/protein deacetylases. *Biochemistry* **2004**, *43*, 9877−9887.
(45) Jin, L.; Wei, W. T.; Jiang, Y. B.; Peng, H.; Cai, J. H.; Mao, C.; Dai, H.; Choy, W.; Bemis, J. E.; Jirousek, M. R.; Milne, J. C.; Westphal, C. H.; Perni, R. B. Crystal structures of human SIRT3 displaying substrate-induced conformational changes. *J. Biol. Chem.* **2009**, *284*, 24394−24405.
(46) Hoff, K. G.; Avalos, J. L.; Sens, K.; Wolberger, C. Insights into the sirtuin mechanism from ternary complexes containing NAD(+) and acetylated peptide. *Structure* **2006**, *14*, 1231−1240.
(47) Disch, J. S.; Evindar, G.; Chiu, C. H.; Blum, C. A.; Dai, H.; Jin, L.; Schuman, E.; Lind, K. E.; Belyanskaya, S. L.; Deng, J. H.; Coppo, F.; Aquilani, L.; Graybill, T. L.; Cuozzo, J. W.; Lavu, S.; Mao, C.; Vlasuk, G. P.; Perni, R. B. Discovery of thieno[3,2-*d*]pyrimidine-6-carboxamides as potent inhibitors of SIRT1, SIRT2, and SIRT3. *J. Med. Chem.* **2013**, *56*, 3666−3679.
(48) Huber, K.; Schemies, J.; Uciechowska, U.; Wagner, J. M.; Rumpf, T.; Lewrick, F.; Suss, R.; Sippl, W.; Jung, M.; Bracher, F. Novel 3-arylideneindolin-2-ones as inhibitors of NAD(+)-dependent histone deacetylases (Sirtuins). *J. Med. Chem.* **2010**, *53*, 1383−1386.
(49) Rotili, D.; Tarantino, D.; Nebbioso, A.; Paolini, C.; Huidobro, C.; Lara, E.; Mellini, P.; Lenoci, A.; Pezzi, R.; Botta, G.; Lahtela-Kakkonen, M.; Poso, A.; Steinkuhler, C.; Gallinari, P.; De Maria, R.; Fraga, M.; Esteller, M.; Altucci, L.; Mai, A. Discovery of salermide-related sirtuin inhibitors: binding mode studies and antiproliferative effects in cancer cells including cancer stem cells. *J. Med. Chem.* **2012**, *55*, 10937−10947.
(50) Medda, F.; Russell, R. J. M.; Higgins, M.; McCarthy, A. R.; Campbell, J.; Slawin, A. M. Z.; Lane, D. P.; Lain, S.; Westwood, N. J. Novel cambinol analogs as sirtuin inhibitors: synthesis, biological evaluation, and rationalization of activity. *J. Med. Chem.* **2009**, *52*, 2673−2682.
(51) Neugebauer, R. C.; Uchiechowska, U.; Meier, R.; Hruby, H.; Valkov, V.; Verdin, E.; Sippl, W.; Jung, M. Structure−activity studies on splitomicin derivatives as sirtuin inhibitors and computational prediction of binding mode. *J. Med. Chem.* **2008**, *51*, 1203−1213.
(52) Gertz, M.; Fischer, F.; Nguyen, G. T.; Lakshminarasimhan, M.; Schutkowski, M.; Weyand, M.; Steegborn, C. Ex-527 inhibits sirtuins by exploiting their unique NAD+-dependent deacetylation mechanism. *Proc. Natl. Acad. Sci. U. S. A.* **2013**, *110*, E2772−2781.
(53) Finnin, M. S.; Donigian, J. R.; Pavletich, N. P. Structure of the histone deacetylase SIRT2. *Nature Struct. Biol.* **2001**, *8*, 621−625.
(54) Moniot, S.; Schutkowski, M.; Steegborn, C. Crystal structure analysis of human Sirt2 and its ADP−ribose complex. *J. Struct. Biol.* **2013**, *182*, 136−143.
(55) Yamagata, K.; Goto, Y.; Nishimasu, H.; Morimoto, J.; Ishitani, R.; Dohmae, N.; Takeda, N.; Nagai, R.; Komuro, I.; Suga, H.; Nureki, O. Structural basis for potent inhibition of SIRT2 deacetylase by a macrocyclic peptide inducing dynamic structural change. *Structure* **2014**, *22*, 345−352.
(56) Zhao, X.; Allison, D.; Condon, B.; Zhang, F. Y.; Gheyi, T.; Zhang, A. P.; Ashok, S.; Russell, M.; MacEwan, I.; Qian, Y. W.; Jamison, J. A.; Luz, J. G. The 2.5 Å crystals of the SIRT1 catalytic domain bound to nicotinamide adenine dinucleotide (NAD(+)) and an indole (EX527 analogue) reveals a novel mechanism of histone deacetylase inhibition. *J. Med. Chem.* **2013**, *56*, 963−969.
(57) Thompson, J. D.; Higgins, D. G.; Gibson, T. J. Clustal-W—improving the sensitivity of progressive multiple sequence alignment through sequence weighting, position-specific gap penalties and weight matrix choice. *Nucleic Acids Res.* **1994**, *22*, 4673−4680.
(58) Avalos, J. L.; Boeke, J. D.; Wolberger, C. Structural basis for the mechanism and regulation of Sir2 enzymes. *Mol. Cell* **2004**, *13*, 639−648.
(59) Wilcken, R.; Zimmermann, M. O.; Lange, A.; Joerger, A. C.; Boeckler, F. M. Principles and applications of halogen bonding in medicinal chemistry and chemical biology. *J. Med. Chem.* **2013**, *56*, 1363−1388.
(60) McGaughey, G. B.; Gagné, M.; Rappé, A. K. π-Stacking interactions: alive and well in proteins. *J. Biol. Chem.* **1998**, *273*, 15458−15463.
(61) Marsili, S.; Chelli, R.; Schettino, V.; Procacci, P. Thermodynamics of stacking interactions in proteins. *Phys. Chem. Chem. Phys.* **2008**, *10*, 2673−2685.
(62) Friesner, R. A.; Murphy, R. B.; Repasky, M. P.; Frye, L. L.; Greenwood, J. R.; Halgren, T. A.; Sanschagrin, P. C.; Mainz, D. T. Extra precision glide: docking and scoring incorporating a model of hydrophobic enclosure for protein−ligand complexes. *J. Med. Chem.* **2006**, *49*, 6177−6196.
(63) The docking was performed using the Glide docking tool as implemented in the Schrödinger software.
(64) Mellini, P.; Kokkola, T.; Suuronen, T.; Salo, H. S.; Tolvanen, L.; Mai, A.; Lahtela-Kakkonen, M.; Jarho, E. M. Screen of pseudopeptidic inhibitors of human Sirtuins 1−3: two lead compounds with antiproliferative effects in cancer cells. *J. Med. Chem.* **2013**, *56*, 6681−6695.
(65) Smith, B. C.; Denu, J. M. Mechanism-based inhibition of Sir2 deacetylases by thioacetyl-lysine peptide. *Biochemistry* **2007**, *46*, 14478−14486.
(66) Yoon, Y. K.; Ali, M. A.; Wei, A. C.; Choon, T. S.; Osman, H.; Parang, K.; Shirazi, A. N. Synthesis and evaluation of novel benzimidazole derivatives as sirtuin inhibitors with antitumor activities. *Bioorg. Med. Chem.* **2014**, *22*, 703−710.
(67) North, B. J.; Marshall, B. L.; Borra, M. T.; Denu, J. M.; Verdin, E. The human Sir2 ortholog, SIRT2, is an NAD(+)-dependent tubulin deacetylase. *Mol. Cell* **2003**, *11*, 437−444.
(68) McCarthy, A. R.; Sachweh, M. C. C.; Higgins, M.; Campbell, J.; Drummond, C. J.; van Leeuwen, I. M. M.; Pirrie, L.; Ladds, M. J. G. W.; Westwood, N. J.; Lain, S. Tenovin-D3, a novel small-molecule inhibitor of sirtuin SirT2, increases p21 (CDKN1A) expression in a p53-independent manner. *Mol. Cancer Ther.* **2013**, *12*, 352−360.
(69) Bose, P.; Dai, Y.; Grant, S. Histone deacetylase inhibitor (HDACI) mechanisms of action: emerging insights. *Pharmacol. Ther.* **2014**, *143*, 323−336.
(70) Vaquero, A.; Scher, M. B.; Lee, D. H.; Sutton, A.; Cheng, H. L.; Alt, F. W.; Serrano, L.; Sternglanz, R.; Reinberg, D. SirT2 is a histone deacetylase with preference for histone H4 Lys 16 during mitosis. *Genes Dev.* **2006**, *20*, 1256−1261.
(71) Taillier, C.; Gille, B.; Bellosta, V.; Cossy, J. Synthetic approaches and total synthesis of natural zoapatanol. *J. Org. Chem.* **2005**, *70*, 2097−2108.
(72) Frankowski, K. J.; Golden, J. E.; Zeng, Y. B.; Lei, Y.; Aube, J. Syntheses of the stemona alkaloids (±)-stenine, (±)-neostenine, and (±)-13-epineostenine using a stereodivergent Diels−Alder/azido-Schmidt reaction. *J. Am. Chem. Soc.* **2008**, *130*, 6018−6024.
(73) Kaiser, F.; Schwink, L.; Velder, J.; Schmalz, H. G. Studies toward the total synthesis of mumbaistatin, a highly potent glucose-6-phosphate translocase inhibitor. Synthesis of a mumbaistatin analogue. *J. Org. Chem.* **2002**, *67*, 9248−9256.
(74) Kitbunnadaj, R.; Zuiderveld, O. P.; Christophe, B.; Hulscher, S.; Menge, W. M. P. B.; Gelens, E.; Snip, E.; Bakker, R. A.; Celanire, S.; Gillard, M.; Talaga, P.; Timmerman, H.; Leurs, R. Identification of 4-(1*H*-imidazol-4(5)-ylmethyl)pyridine (immethridine) as a novel, potent, and highly selective histamine H-3 receptor agonist. *J. Med. Chem.* **2004**, *47*, 2414−2417.
(75) Altendorfer, M.; Raja, A.; Sasse, F.; Irschik, H.; Menche, D. Modular synthesis of polyene side chain analogues of the potent macrolide antibiotic etnangien by a flexible coupling strategy based on hetero-bis-metallated alkenes. *Org. Biomol. Chem.* **2013**, *11*, 2116−2139.
(76) Enholm, E.; Joshi, A.; Wright, D. L. Photocurable hard and porous biomaterials from ROMP precursors cross-linked with diyl radicals. *Bioorg. Med. Chem. Lett.* **2005**, *15*, 5262−5265.
(77) Kiviranta, P. H.; Suuronen, T.; Wallén, E. A. A.; Leppänen, J.; Tervonen, J.; Kyrylenko, S.; Salminen, A.; Poso, A.; Jarho, E. M. *N*-epsilon-Thioacetyl-lysine-containing tri-, tetra-, and pentapeptides as SIRT1 and SIRT2 inhibitors. *J. Med. Chem.* **2009**, *52*, 2153−2156.

(78) Kiviranta, P. H.; Leppänen, J.; Rinne, V. M.; Suuronen, T.; Kyrylenko, O.; Kyrylenko, S.; Kuusisto, E.; Tervo, A. J.; Järvinen, T.; Salminen, A.; Poso, A.; Wallén, E. A. A. *N*-(3-(4-Hydroxyphenyl)-propenoyl)-amino acid tryptamides as SIRT2 inhibitors. *Bioorg. Med. Chem. Lett.* **2007**, *17*, 2448−2451.
(79) Tervo, A. J.; Kyrylenko, S.; Niskanen, P.; Salminen, A.; Leppänen, J.; Nyronen, T. H.; Järvinen, T.; Poso, A. An in silico approach to discovering novel inhibitors of human sirtuin type 2. *J. Med. Chem.* **2004**, *47*, 6292−6298.
(80) Hubbard, B. P.; Gomes, A. P.; Dai, H.; Li, J.; Case, A. W.; Considine, T.; Riera, T. V.; Lee, J. E.; Yen, E. S.; Lamming, D. W.; Pentelute, B. L.; Schuman, E. R.; Stevens, L. A.; Ling, A. J. Y.; Armour, S. M.; Michan, S.; Zhao, H. Z.; Jiang, Y.; Sweitzer, S. M.; Blum, C. A.; Disch, J. S.; Ng, P. Y.; Howitz, K. T.; Rolo, A. P.; Hamuro, Y.; Moss, J.; Perni, R. B.; Ellis, J. L.; Vlasuk, G. P.; Sinclair, D. A. Evidence for a common mechanism of SIRT1 regulation by allosteric activators. *Science* **2013**, *339*, 1216−1219.
(81) Heltweg, B.; Gatbonton, T.; Schuler, A. D.; Posakony, J.; Li, H. Z.; Goehle, S.; Kollipara, R.; DePinho, R. A.; Gu, Y. S.; Simon, J. A.; Bedalov, A. Antitumor activity of a small-molecule inhibitor of human silent information regulator 2 enzymes. *Cancer Res.* **2006**, *66*, 4368−4377.